

# Rare-element granitic pegmatite of Miocene age emplaced in UHP rocks from Visole, Pohorje Mountains (Eastern Alps, Slovenia): accessory minerals, monazite and uraninite chemical dating

PAVEL UHER<sup>1</sup>, MARIAN JANÁK<sup>1</sup>, PATRIK KONEČNÝ<sup>2</sup> and MIRIJAM VRABEC<sup>3</sup>

<sup>1</sup>Geological Institute, Slovak Academy of Sciences, Dúbravská cesta 9, 840 05 Bratislava, Slovak Republic; puher@fns.uniba.sk; marian.janak@savba.sk

<sup>2</sup>Dionýz Štúr State Geological Institute, Mlynská dolina 1, 817 04 Bratislava, Slovak Republic; patrik.konecny@geology.sk

<sup>3</sup>University of Ljubljana, Faculty of Natural Sciences and Engineering, Department of Geology, Aškerčeva 12, SI-1000 Ljubljana, Slovenia

(Manuscript received October 30, 2013; accepted in revised form March 11, 2014)

**Abstract:** The granitic pegmatite dike intruded the Cretaceous UHP rocks at Visole, near Slovenska Bistrica, in the Pohorje Mountains (Slovenia). The rock consists mainly of K-feldspar, albite and quartz, subordinate muscovite and biotite, while the accessory minerals include spessartine-almandine, zircon, ferrocolumbite, fluorapatite, monazite-(Ce), uraninite, and magnetite. Compositions of garnet ( $\text{Sp}_{48-49}\text{Alm}_{45-46}\text{Grs} + \text{And}_{3-4}\text{Prp}_{1.5-2}$ ), metamict zircon with 3.5 to 7.8 wt. %  $\text{HfO}_2$  [atom.  $100\text{Hf}/(\text{Hf} + \text{Zr}) = 3.3 - 7.7$ ] and ferrocolumbite [atom.  $\text{Mn}/(\text{Mn} + \text{Fe}) = 0.27 - 0.43$ ,  $\text{Ta}/(\text{Ta} + \text{Nb}) = 0.03 - 0.46$ ] indicate a relatively low to medium degree of magmatic fractionation, characteristic of the muscovite — rare-element class or beryl-columbite subtype of the rare-element class pegmatites. Monazite-(Ce) reveals elevated Th and U contents ( $\leq 11$  wt. %  $\text{ThO}_2$ ,  $\leq 5$  wt. %  $\text{UO}_2$ ). The monazite-garnet geothermometer shows a possible precipitation temperature of  $\sim 495 \pm 30$  °C at  $P \sim 4$  to 5 kbar. Chemical U-Th-Pb dating of the monazite yielded a Miocene age ( $17.2 \pm 1.8$  Ma), whereas uraninite gave a younger (~14 Ma) age. These ages are contemporaneous with the main crystallization and emplacement of the Pohorje pluton and adjacent volcanic rocks (20 to 15 Ma), providing the first documented evidence of Neogene granitic pegmatites in the Eastern Alps. Consequently, the Visole pegmatite belongs to the youngest rare-element granitic pegmatite populations in Europe, together with the Paleogene pegmatite occurrences along the Periadriatic (Insubric) Fault System in the Alps and in the Rhodope Massif, as well as the Late Miocene to Pliocene pegmatites in the Tuscany magmatic province (mainly on the Island of Elba).

**Key words:** granitic pegmatite, spessartine-almandine, columbite, zircon, fluorapatite, monazite, uraninite, age, Pohorje, Eastern Alps.

## Introduction

Rare-element granitic pegmatites represent lithologically unique rocks, some of the most evolved magmatic rocks on the Earth, and principally the products of extreme magmatic fractionation of parental granitic magma (London 2008, and references therein). The fractionation processes in fluid-rich environments enabled the concentration of a variety of rare lithophile elements (Be, B, Ta, Nb, Li, Rb, Cs, etc.) and precipitation of their own minerals. Rare-element granitic pegmatites usually occur in the Precambrian cratons and ancient collisional zones. However, they are also common in the Paleozoic to Cenozoic continent- and subduction-related collisional terranes. In Europe, the youngest known rare-element and other granitic pegmatites occur in Alpine-orogeny related, post-collisional fault zones between the continental fragments, such as the Periadriatic, Aegean and Corsica-Apulia zones, together with coeval granitic rocks and other related plutonic and volcanic members. The magmatic province along the Periadriatic (Insubric) Fault System comprises Eocene to Oligocene (~42 to 25 Ma; e.g. Scharbert 1975; Romer et al. 1996; Oberli et al. 2004; Lustrino et al. 2011;

Pomella et al. 2011, etc.), mainly tonalite to granodiorite plutonic rocks, which occur in the belt from the Italian Alps (Biella, Bergell, Adamello, Novate intrusions, etc.) to Slovenia (Karavanke Mts). The Oligocene to Miocene granitic rocks of the Pannonian area (Zala basin) and Sáva-Vardar zones as well as the Serbo-Macedonian Massif (Pamić & Balen 2001; Pamić et al. 2002; Benedek 2004; Kovács et al. 2007, and references therein) represent a possible east and south-east continuation of the Periadriatic magmatic province. Occurrences of several late Cretaceous, Paleogene to early Neogene granitic intrusions (~70 to 20 Ma) are reported from the Rhodope Massif in Greece and Bulgaria (e.g. Kiliias & Mountakis 1998; Soldatos et al. 2008; Pipera et al. 2013). In contrast, the monzogranites of the Tuscany province, mainly the Monte Capanne pluton (Elba Island, Italy), are younger in age, Late Miocene to Pliocene intrusions (~8 to 4.3 Ma; Dini et al. 2002; Peccerillo 2005). The Periadriatic, Rhodope, and Tuscany granitic rocks contain associated pegmatite dikes, in some places with rare-element mineralization (e.g. Wenger & Armbruster 1991; Pezzotta 2000; Alexandrov et al. 2001; Aurisicchio et al. 2001, 2002; Guastoni et al. 2008; Guastoni 2012).

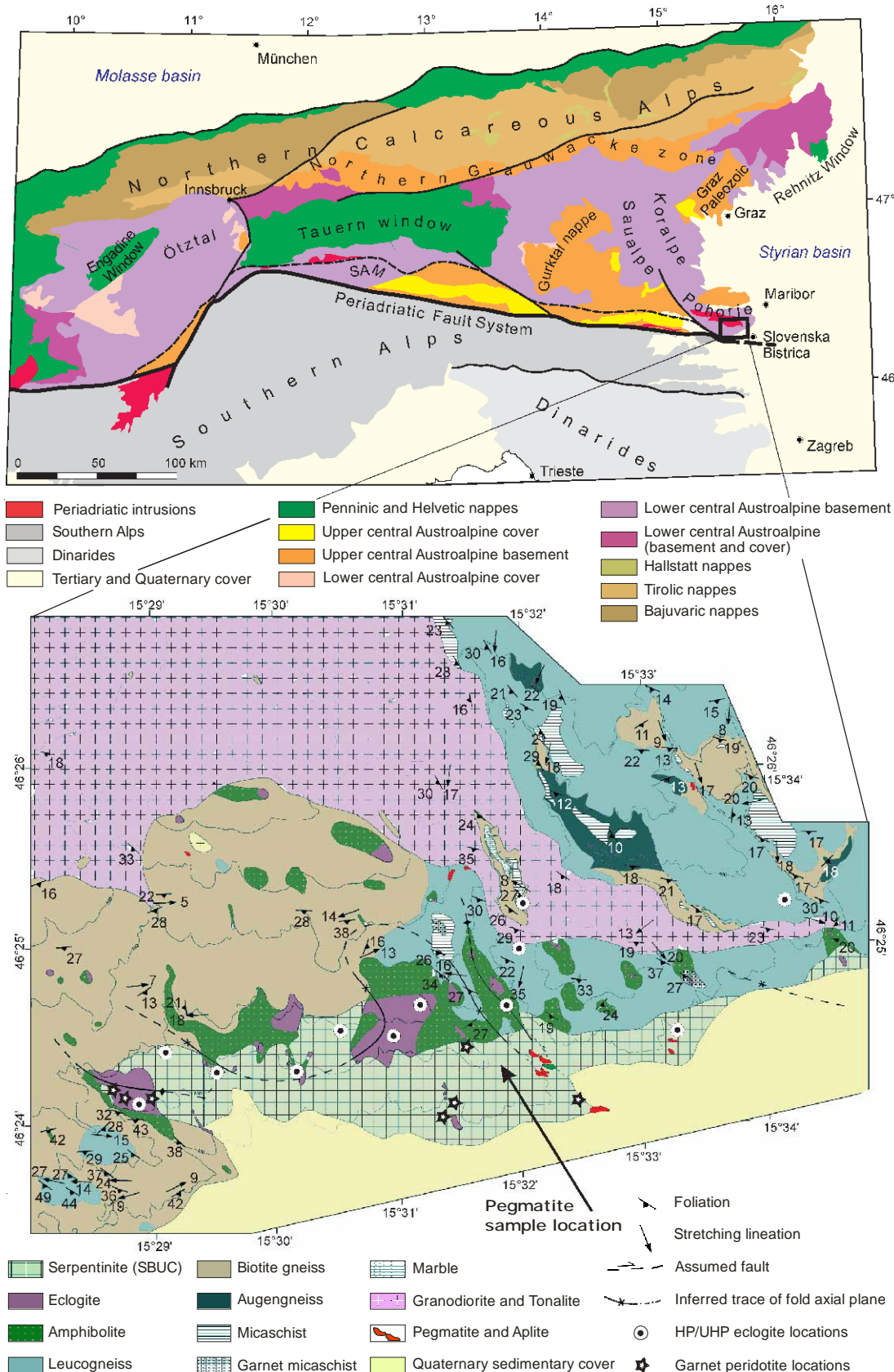


**Fig. 1. Top** — Tectonic map of the Eastern Alps, modified from Neubauer & Höck (2000), Schmid et al. (2004) and Janák et al. (2006). SAM-Southern Border of Alpine Metamorphism after Hoinkes et al. (1999). **Bottom** — Geological map of south-eastern Pohorje modified from Kirst et al. (2010) with sample location.

Dykes of aplites and granitic pegmatites were also described in the Pohorje Mountains (Slovenia), the easternmost continuation of the Alpine, Periadriatic plutonic-volcanic province (e.g. Kirst et al. 2010). They contain tourmaline and beryl in some places (Zupančič et al. 1994; Vrabec & Dolenc 2002). The ages of the plutonic gabbros, tonalites, granodiorites, granitic porphyries and volcanic rocks (mainly dacites) of the Pohorje Mts have been determined as Early to Middle Miocene (20 to 15 Ma; Fodor et al. 2008; Trajanova et al. 2008), younger than other Periadriatic magmatic rocks in the Western and Central Alps. However, a detailed description of the mineral composition, age determination and genetic relations of the Pohorje granitic pegmatites is still lacking.

Consequently, the aim of our contribution is the characterization of a newly discovered rare-element granitic pegmatite near Visole, in the SE part of the Pohorje Mts. Compositional variations of accessory minerals, chemical dating of monazite and uraninite, as well as age relations to adjacent magmatic rocks and other Paleogene to Neogene pegmatite populations in the broader Aegean, Periadriatic and Apulian area are presented.

## Geological background

The Pohorje Mountains in north-eastern Slovenia are located on the south-eastern margin of the Eastern Alps (Fig. 1). The area of the Pohorje Mts is built up of two major tectonic units or nappes emplaced during the Cretaceous. The lower nappe represents the Lower Central Austroalpine (Janák et al. 2004) and consists of medium- to high-grade metamorphic rocks of continental crust, predominantly mica schists, gneisses, marbles and metaquartzites.

In the south-eastern part, numerous eclogite bodies are partly amphibolitized. An 8×1 km body of metatrabasic rocks is located in the vicinity of Slovenska Bistrica (the Slovenska Bistrica Ultramafic Complex, SBUC; Janák et al. 2006) composed of serpentized harzburgite and rarely garnet peridotite (Hinterlechner-Ravnik et al. 1991; Janák et al. 2006; De Hoog et al. 2009, 2011). All these rocks experienced high- to ultrahigh-pressure metamorphism (Hinterlechner-Ravnik et al. 1991; Janák et al. 2004, 2006, 2009; Sassi et al. 2004; Miller et al. 2005; Vrabec et al. 2012) resulting from deep subduction of continental crust (Janák et al. 2004; Stüwe & Schuster 2010). The timing of HP/UHP metamorphism is Cretaceous, ca. 92–93 Ma (Thöni 2002; Miller et al. 2005; Thöni et al. 2008; Janák et al. 2009).

The upper nappe is formed by phyllites and other low-grade metamorphic rocks and their Permo-Triassic sedimentary cover, and represents the Upper Central Austroalpine (Janák et al. 2004). This nappe stack is overlain by Early Miocene sedimentary rocks that belong to the syn-rift basin fill of the Styrian Basin. The Pohorje Mts represent a large antiform with an ESE-WNW-striking axis (Kirst et al. 2010), the core of which is intruded by a granodioritic to tonalitic pluton of Miocene age (~20 to 15 Ma; Altherr et al. 1995; Fodor et al. 2008; Trajanova et al. 2008).

The investigated pegmatite occurs near Visole settlement, ca. 5 km NW of Slovenska Bistrica (Fig. 1). The GPS

geographic coordinates of the pegmatite are as follows: N 46°24.405', E 15°31.590'. The pegmatite forms a dyke, up to ~30 cm thick in serpentinite, within the SBUC. The contacts between the pegmatite and host rock are sharp, without assimilation or desilicification phenomena. The pegmatite body is weakly zonal, the graphic K-feldspar (perthitic microcline to orthoclase)+quartz, coarse-grained to blocky K-feldspar+albite(An<sub>06-08</sub>)+quartz+muscovite+garnet±biotite (Fig. 2a), and fine-grained saccharoidal albite-rich aplitic zones can be distinguished.

## Analytical methods

Polished thin sections of the granitic pegmatite were studied under polarizing microscope.

Chemical compositions and internal zoning of minerals were investigated using the CAMECA SX 100 wave-length electron microprobe housed at the Dionýz Štúr State Geological Institute, Bratislava.

*Spessartine-almandine*, *zircon*, *ferrocolumbite* and *fluorapatite* were measured with electron beam accelerated by 15 kV. Sample current and beam size varied according to minerals: spessartine-almandine was measured with 20 nA and 5 µm beam diameter, zircon and ferrocolumbite with 40 nA and 1–3 µm and fluorapatite with 20 nA and 3–5 µm. The counting times of 10–20 s for main elements and 30–50 s for W, As, Th, U, V, Cr, Sc, Y, and REEs were used. *Monazite-(Ce)* and *uraninite* were also measured with the aim of obtaining age information. Therefore the counting times of U and especially Pb were enlarged to meet requirements for trace element analysis (80 s for U, 300 s for Pb) and the beam current was adjusted to 180 nA and spots were measured with 3 µm beam diameter. The detection limits were 225 and 250 ppm for Th, 205 and 360 ppm for U, 95 and 100 ppm for Pb in monazite and uraninite, respectively. The following standards were used for calibration of all detected minerals: CaWO<sub>4</sub> (W L $\alpha$ ), barite (S K $\alpha$ , Ba L $\alpha$ ), apatite (P K $\alpha$ ), GaAs (As L $\alpha$ ), ferrocolumbite (Nb L $\alpha$ ), LiTaO<sub>3</sub> (Ta L $\alpha$ ), orthoclase (Si K $\alpha$ , K K $\alpha$ ), TiO<sub>2</sub> (Ti K $\alpha$ ), ZrSiO<sub>4</sub> (Si K $\alpha$ , Zr L $\alpha$ ), HfO<sub>2</sub> (Hf L $\alpha$ ), ThO<sub>2</sub> (Th M $\alpha$ ), UO<sub>2</sub> (U M $\beta$ ), Al<sub>2</sub>O<sub>3</sub> (Al K $\alpha$ ), metallic V (V K $\alpha$ ), metallic Cr (Cr K $\alpha$ ), ScPO<sub>4</sub> (Sc K $\alpha$ ), YPO<sub>4</sub> (Y L $\alpha$ ), LaPO<sub>4</sub> (La L $\alpha$ ), CePO<sub>4</sub> (Ce L $\alpha$ ), PrPO<sub>4</sub> (Pr L $\beta$ ), NdPO<sub>4</sub> (Nd L $\beta$ ), SmPO<sub>4</sub> (Sm L $\beta$ ), EuPO<sub>4</sub> (Eu L $\beta$ ), GdPO<sub>4</sub> (Gd L $\alpha$ ), TbPO<sub>4</sub> (Tb L $\alpha$ ), DyPO<sub>4</sub> (Dy L $\beta$ ), HoPO<sub>4</sub> (Ho L $\beta$ ), ErPO<sub>4</sub> (Er L $\beta$ ), TmPO<sub>4</sub> (Tm L $\alpha$ ), YbPO<sub>4</sub> (Yb L $\alpha$ ), LuPO<sub>4</sub> (Lu L $\beta$ ), fayalite (Fe K $\alpha$ ), rhodonite (Mn K $\alpha$ ), willemite (Zn K $\alpha$ ), forsterite (Mg K $\alpha$ ), wollastonite (Ca K $\alpha$ ), PbCO<sub>3</sub> (Pb M $\alpha$ ), albite (Na K $\alpha$ ), LiF (F K $\alpha$ ). We used empirically determined correction factors applied to the following line overlaps: Th→U, Dy→Eu, Gd→Ho, La→Gd, Ce→Gd, Eu→Er, Gd→Er, Sm→Tm, Dy→Lu, Ho→Lu, Yb→Lu, and Dy→As (Konečný et al. 2004). The matrix effects were corrected using the PAP procedure for all the analysed minerals. Spot analyses of monazite and uraninite were corrected for mutual interferences and then the weighted average of apparent ages were calculated following the statistical method of Montel et al. (1996). Moreover, an average age of uraninite was also calculated by the alternative methods of Ranchin (1968), Cameron-Schiman (1978) and Bowles (1990).

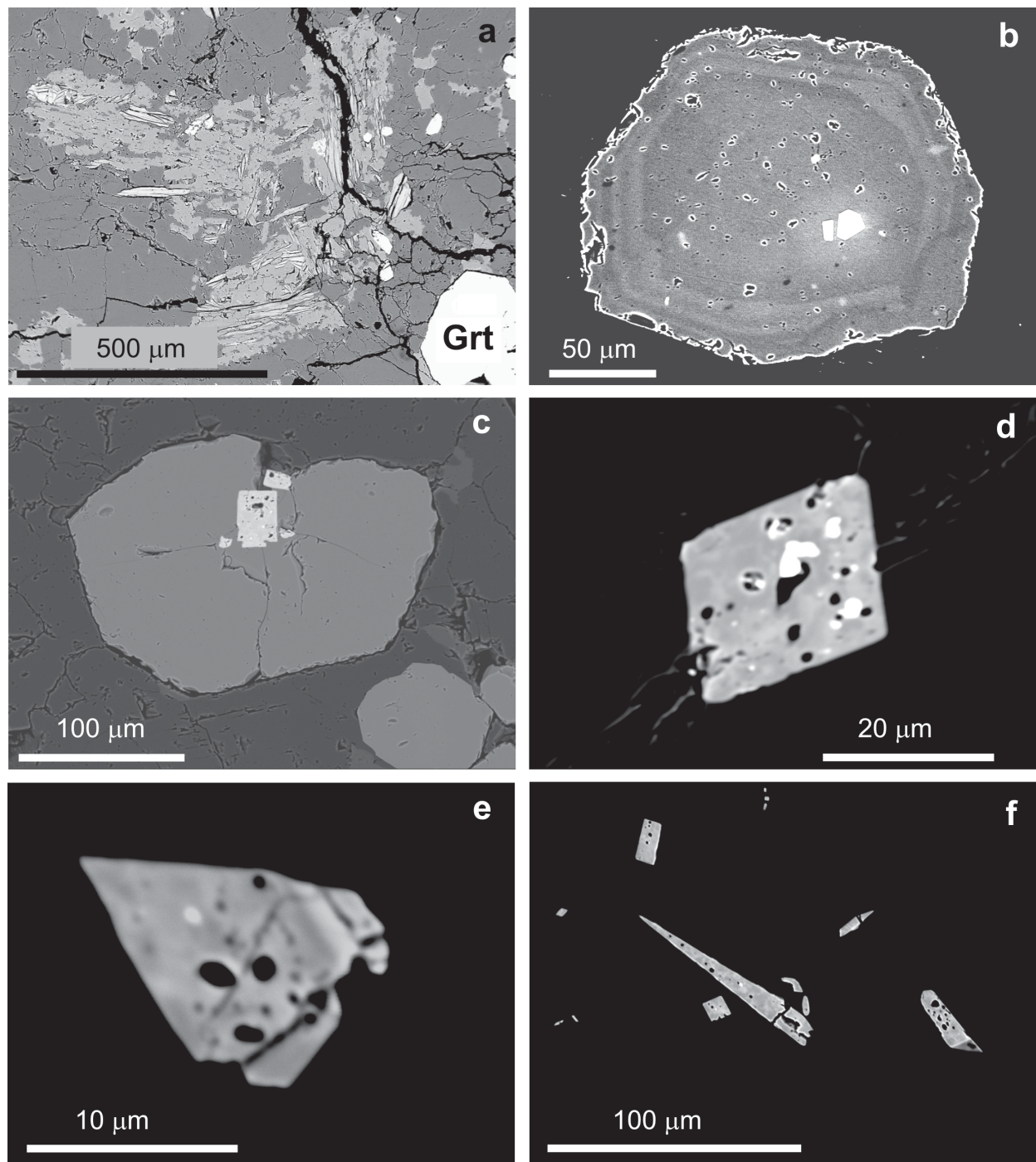


**Fig. 2.** BSE photomicrographs of accessory minerals from the Visole pegmatite. **a** — Coarse-grained quartz-feldspar-mica pegmatite unit with biotite (annite) lamellar crystals in K-feldspar (center) and garnet (Grt); **b** — Spessartine-almandine with oscillatory zoning and two euhedral uraninite inclusions (white) from saccharoidal albite unit; **c** — Spessartine-almandine with zircon inclusions; **d** — Detail of metamict zircon in garnet with anhedral uraninite inclusions (white); **e** — Detail of metamict zircon inclusion in garnet; **f** — Metamict zircon crystals in albite and quartz.

## Results

### Composition of accessory minerals

Spessartine-almandine garnet is the most widespread accessory mineral of the investigated pegmatite. The garnet occurs

as deep ruby red euhedral crystals, usually 0.3 to 1 mm in size, with  $\{211\} > \{110\}$  crystal faces. The garnet forms scattered crystals or groups of several crystals, usually in the aplitic, saccharoidal albite zone. Under BSE, the garnet crystals show nearly regular oscillatory zoning, due to small fluctuations in Fe, Mn and Mg concentration during the crystal growth

**Table 1:** Representative compositions of spessartine-almandine (wt. %) from the Visole pegmatite.

Crystal/position	1/center	1/mid1	1/rim1	2/center	2/mid2	2/rim2
P <sub>2</sub> O <sub>5</sub>	0.00	0.00	0.00	0.00	0.00	0.05
SiO <sub>2</sub>	36.46	36.34	36.75	36.67	36.31	36.33
TiO <sub>2</sub>	0.05	0.04	0.03	0.04	0.04	0.05
Al <sub>2</sub> O <sub>3</sub>	20.02	20.44	20.16	20.05	20.15	20.03
Y <sub>2</sub> O <sub>3</sub>	0.22	0.07	0.00	0.30	0.30	0.08
Fe <sub>2</sub> O <sub>3</sub>	1.46	1.36	0.51	1.02	1.35	1.52
FeO	19.71	20.00	20.42	20.37	20.14	19.98
MnO	21.06	20.72	21.01	21.12	20.71	21.08
ZnO	0.00	0.00	0.00	0.00	0.06	0.08
MgO	0.44	0.45	0.54	0.40	0.45	0.45
CaO	1.42	1.33	1.02	1.10	1.16	1.08
<b>Total</b>	100.84	100.75	100.44	101.07	100.67	100.73
Formulae based on 12 oxygen atoms. 8 cations and valence calculation						
P	0.000	0.000	0.000	0.000	0.000	0.003
Si	2.982	2.970	3.010	2.995	2.976	2.976
Al Z	0.018	0.030	0.000	0.005	0.024	0.021
<b>Sum Z</b>	3.000	3.000	3.010	3.000	3.000	3.000
Ti	0.003	0.002	0.002	0.002	0.002	0.003
Al Y	1.912	1.939	1.946	1.925	1.923	1.913
Fe <sup>3+</sup>	0.090	0.084	0.031	0.063	0.083	0.094
<b>Sum Y</b>	2.005	2.025	1.979	1.990	2.008	2.010
Y	0.010	0.003	0.000	0.013	0.013	0.003
Fe <sup>2+</sup>	1.348	1.367	1.399	1.391	1.380	1.369
Mn	1.459	1.434	1.457	1.461	1.438	1.463
Zn	0.000	0.000	0.000	0.000	0.004	0.005
Mg	0.054	0.055	0.066	0.049	0.055	0.055
Ca	0.124	0.116	0.089	0.096	0.102	0.095
<b>Sum X</b>	2.995	2.975	3.011	3.010	2.992	2.990
Sps	48.9	48.3	48.4	48.7	48.3	49.1
Alm	45.2	46.0	46.5	46.4	46.4	45.9
Prp	1.8	1.9	2.2	1.6	1.8	1.8
Grs+And	4.2	3.9	3.0	3.2	3.4	3.2
<b>Sum</b>	100.0	100.0	100.0	100.0	100.0	100.0
<b>Mn/(Mn+Fe<sup>2+</sup>)</b>	0.52	0.51	0.51	0.51	0.51	0.52

(Fig. 2b). In some places, small zircon and uraninite inclusions were observed in the garnet crystals (Fig. 2b-e).

The garnet crystals are without distinct compositional variations or trends in the main elements (Si, Al, Fe, Mn, Mg and Ca) from core to rim. Analyses of garnet (Table 1) show spessartine-almandine composition with slight dominance of spessartine over almandine and negligible grossular, andradite and pyrope end-members: spessartine attains 48 to 49, almandine 45 to 46, grossular + andradite 3 to 4, and pyrope 1.5 to 2 mol %, the atomic Mn/(Mn+Fe<sup>2+</sup>) ratio attains 0.51 to 0.52 (Table 1). However, central parts of the spessartine-almandine garnet are slightly enriched in Y (0.005 to 0.013 apfu; 0.1 to 0.3 wt. % Y<sub>2</sub>O<sub>3</sub>), whereas the rims are usually without detectable amounts of Y ( $\leq 0.08$  wt. % Y<sub>2</sub>O<sub>3</sub>). Concentrations of other measured elements in the garnet (P, Ti, Sc, V, Cr, Zn, Na) are very low or under the detection limit of the EMPA (<0.1 wt. % of oxide or  $\leq 0.005$  apfu).

*Zircon* forms rare euhedral crystals, usually 5 to 80  $\mu$ m across, as inclusions in the central parts of spessartine-almandine (Fig. 2c-e), or scattered crystals in albite, K-feldspar or quartz (Fig. 2f). Zircon in some places shows slightly irregular zoning, probably due to metamictization. Locally, tiny anhedral inclusions of uraninite (under 2  $\mu$ m in size) were detected in zircon crystals (Fig. 2d). The zircon crystals are enriched in

hafnium; they contain 3.5 to 7.8 wt. % HfO<sub>2</sub> (0.03 to 0.07 Hf apfu), atomic 100Hf/(Hf+Zr) ratio attains 3.3 to 7.7 (Table 2). Uranium concentrations vary between 0.4 and 2.6 wt. % UO<sub>2</sub> (0.003 to 0.018U apfu). The slightly elevated contents of yttrium, 0.1 to 0.7 wt. % Y<sub>2</sub>O<sub>3</sub> ( $\leq 0.012$  Y apfu) and iron, up to 1.1 wt. % Fe<sub>2</sub>O<sub>3</sub> ( $\leq 0.03$  Fe apfu) are also noteworthy. Consequently, zircon and garnet belong to the main mineral carriers of Y and probably also HREEs in the Visole pegmatite.

*Ferrocolumbite* forms euhedral to subhedral crystals of tabular shape in K-feldspar, albite and quartz, usually 15 to 100  $\mu$ m across. The mineral shows two principal types of internal zoning, visible under BSE images: (1) regular fine-scale (<5  $\mu$ m) oscillatory zoning and (2) irregular convolute or mosaic zoning (Fig. 3a-d). Both the regular and irregular zoning reflected mainly Ta-Nb variations in ferrocolumbite. The compositional trend of primary, regular oscillatory zoning in ferrocolumbite crystals is ambiguous: both increasing and decreasing of the Ta/Nb ratio from central to rim zones was observed, whereas the Mn/Fe ratio is nearly constant (Table 3, Fig. 4a). The compositional variations of both textural patterns reveal a distinctly Fe and Nb dominant ferrocolumbite with relatively very low to moderate Mn and Ta contents. The primary ferrocolumbite domains with regular oscillatory zoning show a more uniform Mn/(Mn+Fe) ratio (0.29 to 0.35), but a variable and generally higher Ta/(Ta+Nb) ratio (0.11 to 0.29) in comparison to the secondary irregular domains, where Mn/(Mn+Fe) ratio attains 0.27 to 0.43 and Ta/(Ta+Nb) achieves 0.03 to 0.24 (Table 3, Fig. 4a). Concentrations of other elements are relatively low and similar for both textural types of ferrocolumbite; the mineral contains 0.7 to 2.3 wt. % TiO<sub>2</sub> (0.03 to 0.10 apfu Ti), 0.1 to 0.5 wt. % ZrO<sub>2</sub> ( $\leq 0.014$  apfu Zr), and 0.1 to 0.4 wt. %

MgO ( $\leq 0.034$  apfu Mg). Concentrations of other measured elements (W, Sn, Th, U, Sc, Y, La, Ce, Sb, Zn, Ca, Na) are negligible or under the detection limit of the electron microprobe, generally  $\leq 0.05$  wt. % (Table 3). The charge balance calculated formulae of ferrocolumbite indicate a presence of trivalent iron: Fe<sup>3+)/(Fe<sup>3+</sup>+Fe<sup>2+</sup>) ratio attains 12 atomic % on average. The compositional variations of ferrocolumbite reflect single monovalent substitutions: TaNb<sub>-1</sub>, MnFe<sup>2+</sup><sub>-1</sub>, MgFe<sup>2+</sup><sub>-1</sub>, as well as coupled Ti<sub>3</sub>(Fe<sup>2+</sup>,Mn,Mg)<sub>-1</sub>(Nb,Ta)<sub>-2</sub> and/or Fe<sup>3+</sup>Ti(Fe<sup>2+</sup>,Mn,Mg)<sub>-1</sub>(Nb,Ta)<sub>-1</sub> substitution (Fig. 4b).</sup>

*Fluorapatite* forms euhedral to subhedral columnar crystals, usually 150 to 250  $\mu$ m in size, in association with albite, K-feldspar, biotite, spessartine-almandine, and zircon (Fig. 3e). Fluorapatite crystals are relatively homogeneous, they show nearly end-member composition, where F/(F+OH) atomic ratio attains 0.93 to 1. Elevated Mn concentrations substitution (up to 1.4 wt. % MnO,  $\leq 0.10$  apfu Mn) document MnCa<sub>-1</sub> substitution, negligible Y, Fe and Na contents were also detected (Table 4).

*Monazite-(Ce)* forms individual euhedral to subhedral crystals, usually 10 to 100  $\mu$ m across, in association with quartz, feldspar and muscovite. The monazite crystals are relatively homogenous or they show compositional zoning

**Table 2:** Representative compositions of zircon (wt. %) from the Visole pegmatite.

Crystal/Position	1/center	2/center	3/center	4/center	4/rim	6/center	7/rim
P <sub>2</sub> O <sub>5</sub>	0.16	0.55	0.35	0.31	0.20	0.12	0.31
As <sub>2</sub> O <sub>5</sub>	0.19	0.19	0.20	0.19	0.33	0.19	0.19
SiO <sub>2</sub>	33.12	32.67	31.99	32.14	32.05	32.17	31.84
ZrO <sub>2</sub>	61.63	59.98	59.86	58.47	54.42	59.71	58.43
HfO <sub>2</sub>	3.77	3.62	3.65	3.49	7.83	3.73	3.49
ThO <sub>2</sub>	0.00	0.00	0.00	0.06	0.06	0.00	0.05
UO <sub>2</sub>	0.39	1.46	1.31	2.41	2.56	0.82	2.51
Al <sub>2</sub> O <sub>3</sub>	0.00	0.00	0.00	0.09	0.08	0.00	0.04
Fe <sub>2</sub> O <sub>3</sub>	0.00	0.00	0.00	0.87	0.79	0.97	1.04
Sc <sub>2</sub> O <sub>3</sub>	0.00	0.04	0.03	0.00	0.00	0.00	0.00
Y <sub>2</sub> O <sub>3</sub>	0.10	0.72	0.46	0.47	0.35	0.11	0.51
Ce <sub>2</sub> O <sub>3</sub>	0.09	0.00	0.00	0.00	0.00	0.09	0.00
Er <sub>2</sub> O <sub>3</sub>	0.29	0.32	0.28	0.38	0.37	0.25	0.29
Yb <sub>2</sub> O <sub>3</sub>	0.13	0.10	0.13	0.24	0.14	0.13	0.05
CaO	0.00	0.03	0.03	0.00	0.07	0.00	0.00
<b>Total</b>	99.87	99.68	98.29	99.12	99.25	98.26	98.75
Formulae based on 4 oxygen atoms							
P	0.004	0.014	0.009	0.008	0.005	0.003	0.008
As	0.003	0.003	0.003	0.003	0.006	0.003	0.003
Si	1.022	1.014	1.010	1.011	1.023	1.014	1.007
Zr	0.928	0.908	0.922	0.897	0.847	0.917	0.901
Hf	0.033	0.032	0.033	0.031	0.071	0.034	0.031
Th	0.000	0.000	0.000	0.000	0.000	0.000	0.000
U	0.003	0.010	0.009	0.017	0.018	0.006	0.018
Al	0.000	0.000	0.000	0.003	0.003	0.000	0.001
Fe	0.000	0.000	0.000	0.021	0.019	0.023	0.025
Sc	0.000	0.001	0.001	0.000	0.000	0.000	0.000
Y	0.002	0.012	0.008	0.008	0.006	0.002	0.009
Ce	0.001	0.000	0.000	0.000	0.000	0.001	0.000
Er	0.003	0.003	0.003	0.004	0.004	0.002	0.003
Yb	0.001	0.001	0.001	0.002	0.001	0.001	0.000
Ca	0.000	0.001	0.001	0.000	0.002	0.000	0.000
<b>Sum cat.</b>	2.000	2.000	2.000	2.007	2.007	2.006	2.007
<b>100Hf/(Hf+Zr)</b>	3.43	3.40	3.46	3.34	7.73	3.58	3.33

with irregular mosaic domains or nearly regular to irregular concentric zonal pattern (Fig. 3f), due to variations of Th, U, REEs and Ca concentrations. Moderate to relatively high Th and U contents (~2 to 11 wt. % ThO<sub>2</sub> and ~1 to 5 wt. % UO<sub>2</sub>) are characteristic features of the monazite (Table 5). The monazite represents a common Ce-dominant member with Ce > Nd ≥ La > Sm, Gd, Y, Pr > other REEs atomic proportions (Table 5). Monazite displays relatively large variations of La/Nd (0.36 to 1.02), La/Sm (0.53 to 2.78), La/Gd (0.71 to 4.23) and La/Y (0.91 to 15.7) atomic ratios. The cheralite-type substitution [Ca(Th,U)(REE,Y)<sub>-2</sub>] is the dominant exchange trend; it prevails over the huttonite-type substitution [(Th,U)Si(REE,Y)<sub>-1</sub>(P,As)<sub>-1</sub>] (Fig. 5). Very distinct negative Eu-anomaly is typical for studied monazite, an average Eu/Eu\* ratio achieves 0.015 (Fig. 6).

*Uraninite* occurs as rare euhedral inclusions, up to 15 µm across, in albite and garnet or anhedral inclusions in zircon, up to 5 µm across (Fig. 2b,d,f). Uraninite crystals are compositionally homogeneous with elevated content of Th (2.5 to 3.7 wt. % ThO<sub>2</sub>, 0.025 to 0.037 Th apfu) and they are slightly enriched in Y, REEs, As, Pb and locally also Fe (Table 6). Thorium shows a negative correlation to U (Fig. 7), indicating thorianite-type substitution (ThU<sub>-1</sub>) in uraninite.

*Magnetite* was identified by EDS as scattered euhedral crystals in K-feldspar or saccharoidal albite, in association with garnet.

### Monazite–garnet geothermometry

Measured yttrium concentrations in monazite and garnet, calcium content in garnet and adjacent albite, and calculated X<sub>OH</sub> in fluorapatite, together with estimated pressure and fH<sub>2</sub>O of the Visole pegmatite were used to determine the temperature conditions employing the monazite–garnet thermometer (Pyle et al. 2001). The pressure of the pegmatite emplacement was estimated as 4–5 kbar, consistent with emplacement of adjacent granitic rocks of the Pohorje pluton according to the Al-in-hornblende barometer (Altherr et al. 1995; Fodor et al. 2008). Relevant fH<sub>2</sub>O (~1500 to 2100 bar) was calculated according to Holland & Powell (1998). The calculated temperatures attain ~495 ± 30 °C for the central as well as rim parts of the garnet crystals.

### Chemical dating of monazite and uraninite

Dating of monazite and uraninite based on high Th and/or U content, together with measurable amounts of Pb and negligible content of common, non-radiogenic lead (Bowles 1990; Montel et al. 1996, and references therein) has been applied to determine the age of the Visole pegmatite. Concentrations of U, Th and Pb in monazite and uraninite were measured using the electron microprobe as described above, and the age was calculated according to the Montel et al. (1996) and Konečný et al. (2004) procedure. The resulting age is the weighted average of a group of apparent ages (from point analysis). All measured and calculated data are given in Table 7 and Fig. 8.

The results of monazite dating show an average age of 17.2 ± 1.8 Ma, obtained from 48 spot analyses (Fig. 7). Dating of uraninite shows an average age of 14.2 ± 0.2 Ma (9 measurements). Similar average ages have been obtained from alternative methods of uraninite age calculations, namely 14.5 ± 0.3 Ma of Ranchin (1968), 12.5 ± 0.5 Ma of Cameron-Schiman (1978), and 13.9 ± 0.3 Ma of Bowles (1990).

## Discussion

### Mineral composition

The investigated accessory minerals (spessartine-almandine, zircon, ferrocolumbite, fluorapatite, monazite-(Ce), uraninite) represent an assemblage which belongs to the muscovite — rare-element class or the most primitive, beryl type and beryl-columbite subtype within the rare-element class of granitic pegmatites, according to the recent classification of Černý & Ercit (2005). Beryl, as the index mineral of this subtype was not identified in the studied Visole peg-

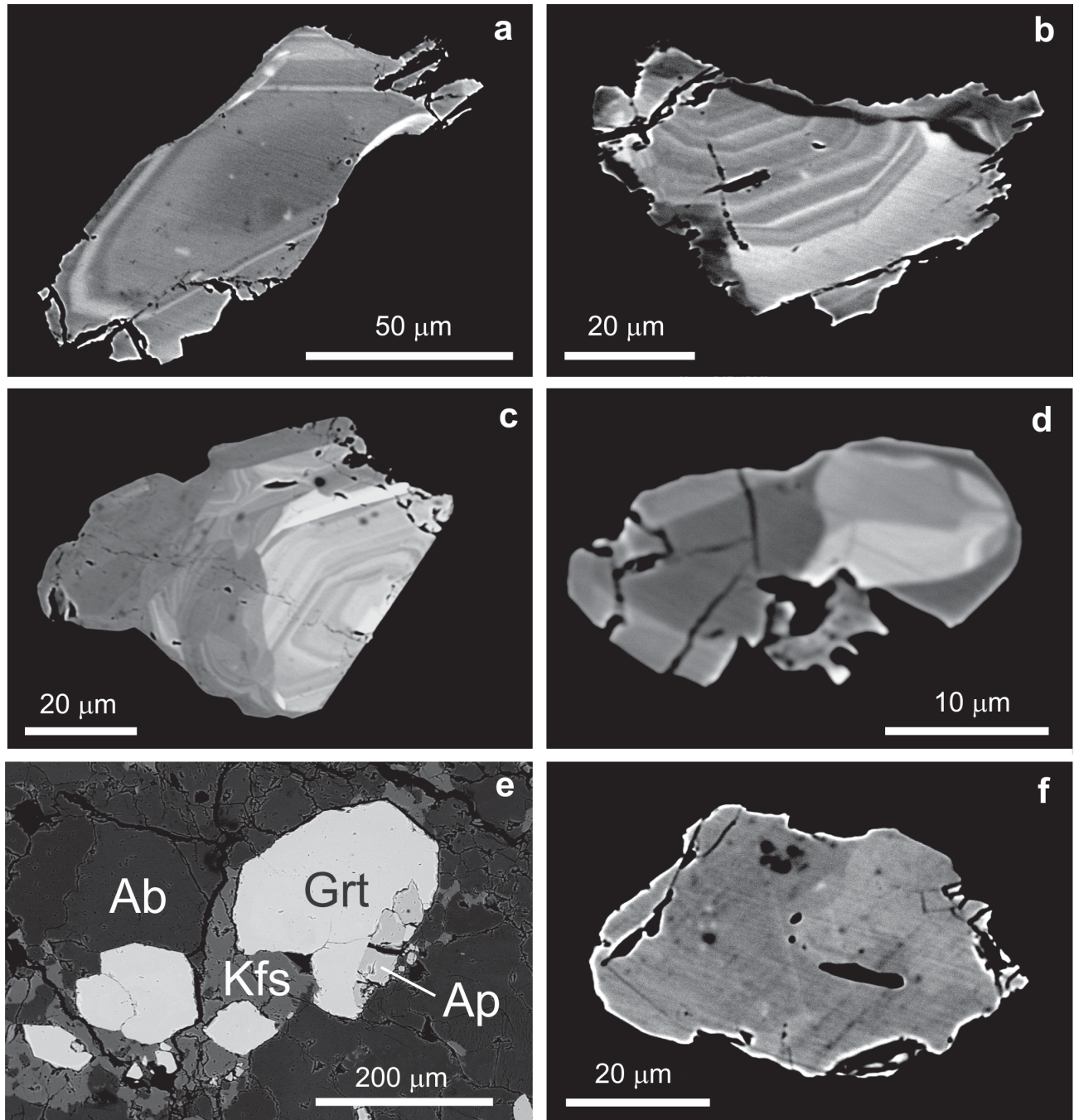


**Fig. 3.** BSE photomicrographs of accessory minerals from the Visole pegmatite. **a-d** — Ferrocolumbite with primary, regular oscillatory zoning and secondary, irregular convolute and mosaic zoning; **e** — Fluorapatite (Ap) in association with garnet (Grt), K-feldspar (Kfs) and albite (Ab); **f** — Crystal of monazite-(Ce) with irregular zoning.

matite. However, beryl and tourmaline were noted in some granitic pegmatites of the Pohorje Mountains (Zupančič et al. 1994; Vrabec & Dolenc 2002).

*Spessartine-almandine* garnet is a characteristic accessory phase of peraluminous crustal leucogranite-pegmatite suites of S-type affinity (e.g. Baldwin & von Knorring 1983; Whitworth 1992; London 2008; Wise & Brown 2010; Černý et al. 2012). The Mn/(Mn+Fe) ratio and Mg+Ca content of the pegmatitic garnet indicate the degree of magmatic fractionation

of the parental pegmatite body. Generally, the Mn/(Mn+Fe) ratio increases and Mg+Ca decreases in the more evolved rare-element, especially complex Li-Cs- bearing granitic pegmatites in comparison to poorly evolved rare-element (beryl type), muscovite — rare-element, and especially barren pegmatites (Černý et al. 1985; London 2008, and references therein). The uniform Fe/(Fe+Mn) ratio (0.51 to 0.52) as well as low Mg and Ca concentrations in spessartine-almandine from the Visole pegmatite ( $\leq 4$  mol % gross-

**Table 3:** Representative compositions of primary and secondary domains of ferrocolumbite (wt. %) from the Visole pegmatite

Population	Primary	Primary	Primary	Primary	Second.	Second.	Second.	Second.
Crystal/Anal.	1.1	1.3	1.6	3.2	1.7	1.12	2.1	3.7
WO <sub>3</sub>	0.00	0.00	0.00	0.00	0.13	0.00	0.00	0.00
Nb <sub>2</sub> O <sub>5</sub>	47.24	55.69	33.20	64.01	51.13	73.33	60.32	67.68
Ta <sub>2</sub> O <sub>5</sub>	31.76	22.85	46.53	13.94	27.29	4.41	17.60	10.84
TiO <sub>2</sub>	1.67	1.59	1.47	1.98	1.76	1.44	1.65	1.19
SnO <sub>2</sub>	0.00	0.00	0.00	0.00	0.00	0.00	0.00	0.00
ZrO <sub>2</sub>	0.35	0.14	0.14	0.15	0.10	0.00	0.47	0.06
UO <sub>2</sub>	0.16	0.17	0.09	0.14	0.11	0.00	0.10	0.08
Sc <sub>2</sub> O <sub>3</sub>	0.00	0.06	0.06	0.08	0.07	0.07	0.00	0.00
Ce <sub>2</sub> O <sub>3</sub>	0.08	0.06	0.00	0.11	0.08	0.00	0.00	0.00
Fe <sub>2</sub> O <sub>3</sub>	2.40	2.50	2.39	1.34	3.38	1.96	2.14	0.02
FeO	10.95	11.28	9.87	11.98	10.66	13.11	11.59	11.10
MnO	5.28	5.85	5.14	6.45	5.45	5.92	6.28	8.40
ZnO	0.00	0.00	0.00	0.08	0.09	0.00	0.00	0.00
MgO	0.30	0.22	0.20	0.18	0.26	0.29	0.14	0.25
<b>Total</b>	100.19	100.41	99.09	100.44	100.51	100.53	100.29	99.62
Formulae based on 3 cations, 6 O atoms and valence calculation								
W	0.000	0.000	0.000	0.000	0.002	0.000	0.000	0.000
Nb	1.353	1.530	1.032	1.694	1.427	1.863	1.624	1.791
Ta	0.547	0.378	0.870	0.222	0.458	0.067	0.285	0.173
Ti	0.080	0.073	0.076	0.087	0.082	0.061	0.074	0.052
Sn	0.000	0.000	0.000	0.000	0.000	0.000	0.000	0.000
Zr	0.011	0.004	0.005	0.004	0.003	0.000	0.014	0.002
Sc	0.000	0.003	0.004	0.004	0.004	0.003	0.000	0.000
<b>Sum B</b>	1.991	1.988	1.987	2.011	1.976	1.994	1.997	2.018
U	0.002	0.002	0.001	0.002	0.002	0.000	0.001	0.001
Ce	0.002	0.001	0.000	0.002	0.002	0.000	0.000	0.000
Fe <sup>3+</sup>	0.114	0.114	0.124	0.059	0.157	0.083	0.096	0.001
Fe <sup>2+</sup>	0.580	0.573	0.568	0.586	0.551	0.616	0.577	0.543
Mn	0.283	0.301	0.299	0.320	0.285	0.282	0.317	0.416
Zn	0.000	0.000	0.000	0.003	0.004	0.000	0.000	0.000
Mg	0.028	0.020	0.021	0.016	0.024	0.024	0.012	0.022
<b>Sum A</b>	1.009	1.011	1.013	0.988	1.025	1.005	1.003	0.983
Mn/(Mn+Fe)	0.290	0.305	0.302	0.332	0.287	0.287	0.320	0.433
Ta/(Ta+Nb)	0.288	0.198	0.457	0.116	0.243	0.035	0.149	0.088

sular + andradite, and  $\leq 2$  mol % pyrope molecule) is analogous to the garnets in (muscovite)-rare-element granitic pegmatites (e.g. Gbelský 1980; Baldwin & von Knorring 1983; Černý et al. 1985; Wise & Brown 2010). The relatively uniform and homogeneous compositions of spessartine-almandine crystals without any distinct compositional variations or trends from center to rims and weak oscillatory zoning illustrate only small fluctuations in Fe, Mn and other elements during the relatively rapid and short crystal growth.

Besides slightly elevated Y content, the chemical composition of zircon from the Visole pegmatite also shows Hf-enrichment (up to 7.8 wt. % HfO<sub>2</sub>) and U (up to 2.6 wt. % UO<sub>2</sub>), which is a typical feature of zircon in evolved granitic pegmatites and highly fractionated leucogranites (e.g. Černý et al. 1985; Uher & Černý 1998; Breiter et al. 2006; Breiter & Škoda 2012).

The degree of Nb-Ta fractionation in ferrocolumbite of the Visole pegmatite is low to moderate as shown by the clear predominance of Fe/(Fe+Nb) and Ta/(Ta+Nb) ratios (0.27 to 0.43 and 0.03 to

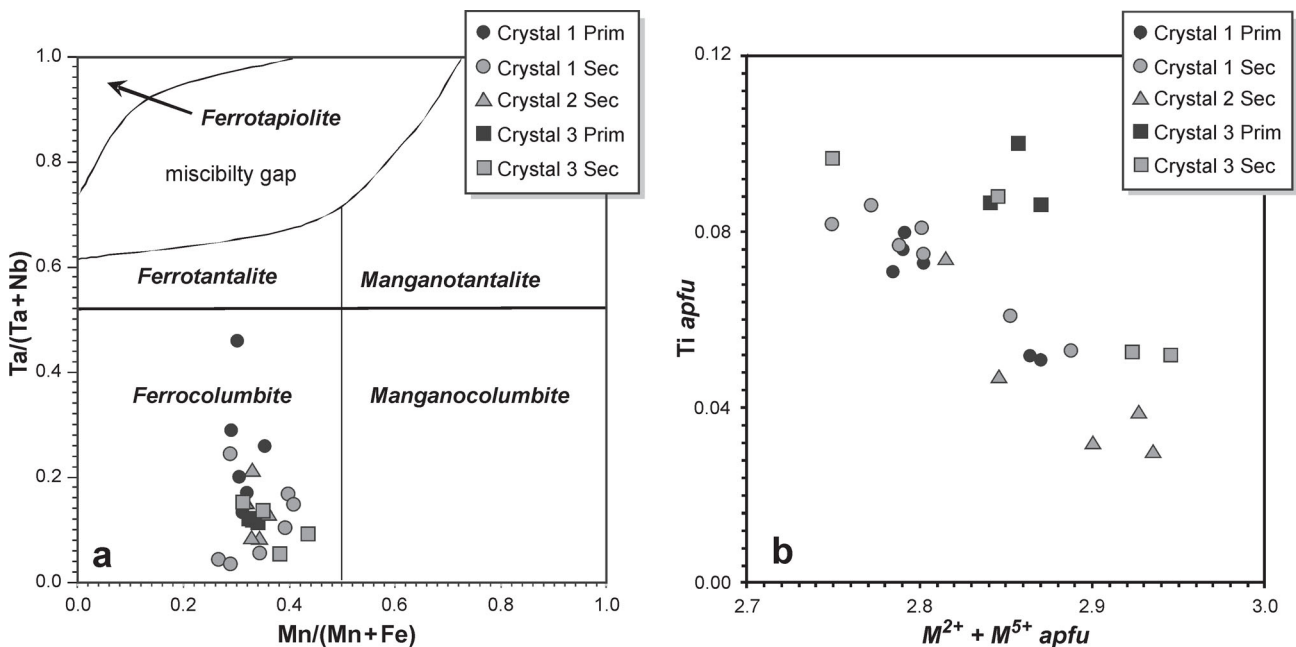


**Fig. 4.** Compositional variation of ferrocolumbite from the Visole pegmatite (atomic proportions). **a** — Quadrilateral columbite-tantalite diagram; **b** — Substitution Ti vs.  $M^{2+}$  ( $F\text{ Mn} + \text{Mg}$ ) +  $M^{5+}$  ( $\text{Nb} + \text{Ta}$ ) diagram.

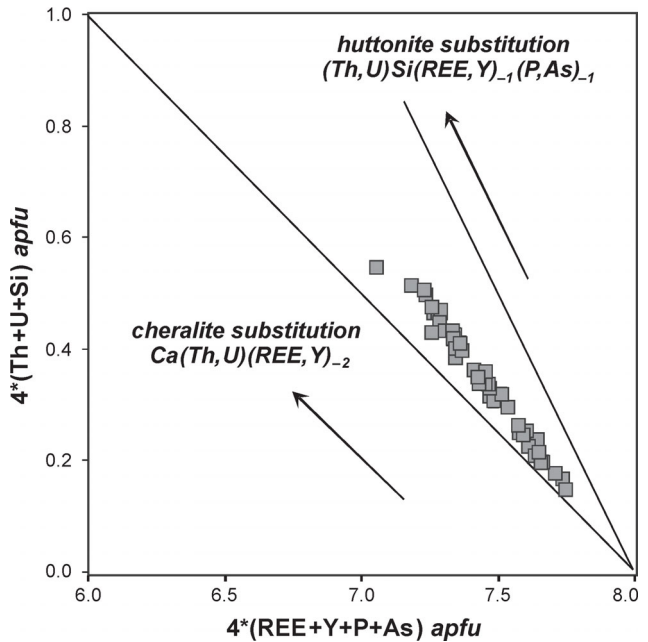
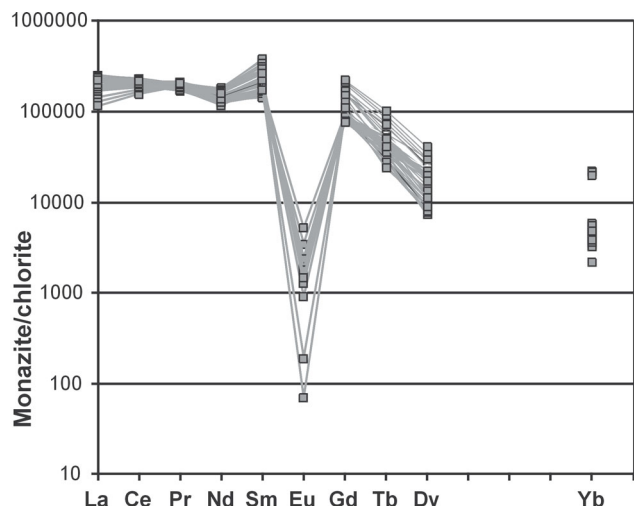
**Table 4:** Representative compositions of fluorapatite (wt. %) from the Visole pegmatite.

Crystal/Position Analyse	X1Core 1	X2Core 2	X2Rim 3
P <sub>2</sub> O <sub>5</sub>	41.38	41.48	41.22
As <sub>2</sub> O <sub>5</sub>	0.08	0.09	0.08
SiO <sub>2</sub>	0.03	0.00	0.09
Y <sub>2</sub> O <sub>3</sub>	0.31	0.27	0.29
Ce <sub>2</sub> O <sub>3</sub>	0.15	0.15	0.11
Nd <sub>2</sub> O <sub>3</sub>	0.14	0.09	0.09
Yb <sub>2</sub> O <sub>3</sub>	0.10	0.00	0.00
FeO	0.21	0.25	0.20
MnO	1.44	0.99	0.88
CaO	52.92	54.32	54.00
Na <sub>2</sub> O	0.20	0.16	0.15
H <sub>2</sub> O*	0.00	0.13	0.10
F	3.83	3.47	3.51
O=F	-1.61	-1.46	-1.48
<b>Total</b>	99.18	99.94	99.24
Formulae based on 13 anions and OH+F = 1 apfu			
P	2.989	2.973	2.972
As	0.004	0.004	0.004
Si	0.003	0.000	0.008
<b>Sum T</b>	2.996	2.977	2.984
Y	0.014	0.012	0.013
Ce	0.005	0.005	0.003
Nd	0.004	0.003	0.003
Yb	0.003	0.000	0.000
Fe	0.015	0.018	0.014
Mn	0.104	0.071	0.063
Ca	4.838	4.927	4.927
Na	0.033	0.026	0.025
<b>Sum M</b>	5.016	5.062	5.048
<b>Sum cat.</b>	8.012	8.039	8.032
OH	0.000	0.071	0.055
F	1.034	0.929	0.945
<b>Sum X</b>	1.034	1.000	1.000
O	11.966	12.071	12.055

\* H<sub>2</sub>O — calculated on ideal stoichiometry S, Al, La, Mg, Sr, Ba, Pb, K, Cl below detection limit.

0.24, respectively). Such values are typical for the most primitive, fluorine-poor populations of beryl-columbite subtype pegmatites, for example in the Separation Rapids group, Ontario (Tindle & Breaks 1998) or Topsham area, Maine (Wise et al. 2012). On the contrary, fractionation trends of the Nb-Ta oxide minerals in more evolved beryl-columbite pegmatites also attain Ta- and Mn-rich members of the columbite, tapiolite and wodginitic group minerals (Černý et al. 1986; Černý 1989; Tindle & Breaks 1998; Novák et al. 2000, 2003; Chudík et al. 2011). The textural relationships of the Visole ferrocolumbite indicate its complex origin: a primary magmatic character of the regular oscillatory zones, which are partially replaced by younger, late-magmatic to post-magmatic, secondary irregular zones, presumably originating from dissolution-reprecipitation of the primary ferrocolumbite crystals. Such complicated texture of columbite-group minerals reflects a magmatic to subsolidus evolution of the parental rocks as described in many granitic pegmatites (Van Liervelde et al. 2007; Rao et al. 2009; Chudík et al. 2011, etc.).

*Fluorapatite* is the most common phosphate phase in phosphate-poor granitic pegmatites of the LCT family, derived

**Fig. 5.** Monazite-(Ce) Th+U+Si vs. REE+P+As substitution diagram from the Visole pegmatite (atomic proportions).**Fig. 6.** Monazite/chondrite normalized diagram of REE from the Visole pegmatite (weight proportions). Chondrite values after Taylor & McLennan (1985).

from low-P granitic magmas. On the contrary, Fe-Mn-Ca and Li-Na-Al phosphate phases (mainly triplite, graftonite, beusite, sarcophase, prophyllite, amblygonite, montebrasite) are developed in P-rich rare-element granitic pegmatites (e.g. Černý & Ercit 2005; London 2008). Very high F/(F+OH) ratio (>0.9) and elevated Mn content ( $\leq 0.1$  apfu) in the Visole fluorapatite document a slight to moderate degree of magmatic fractionation; the values are very comparable to primary magmatic apatite compositions from numerous granitic pegmatites (Piccoli & Candela 2002, and references therein).

The Eu/Eu\* is distinctly low in the studied monazite (0.015 in average). Such negative Eu-anomalies indicate an

**Table 5:** Representative compositions of monazite-(Ce) (wt. %) from the Visole pegmatite.

Anal.	1	2	3	4	5	6	7	8
P <sub>2</sub> O <sub>5</sub>	29.32	29.32	28.59	29.22	29.57	28.31	28.73	28.70
As <sub>2</sub> O <sub>5</sub>	0.11	0.09	0.11	0.12	0.11	0.24	0.23	0.23
SiO <sub>2</sub>	0.64	0.23	0.51	0.43	0.31	0.76	0.39	0.35
ThO <sub>2</sub>	7.58	1.95	7.43	10.94	3.84	9.53	5.28	4.04
UO <sub>2</sub>	2.78	1.65	1.02	2.54	1.10	1.11	4.99	1.20
Y <sub>2</sub> O <sub>3</sub>	4.64	3.03	2.12	1.41	1.50	2.11	1.77	0.49
La <sub>2</sub> O <sub>3</sub>	9.27	5.53	9.86	9.43	7.61	9.54	9.88	9.50
Ce <sub>2</sub> O <sub>3</sub>	21.23	18.52	23.23	21.97	21.60	22.84	23.29	24.17
Pr <sub>2</sub> O <sub>3</sub>	2.73	3.12	3.09	2.80	3.23	3.00	3.06	3.42
Nd <sub>2</sub> O <sub>3</sub>	10.55	15.14	11.68	9.72	14.40	11.15	10.60	13.59
Sm <sub>2</sub> O <sub>3</sub>	3.93	9.82	4.87	4.88	8.38	4.61	4.81	7.27
Eu <sub>2</sub> O <sub>3</sub>	0.02	0.00	0.05	0.02	0.00	0.00	0.00	0.00
Gd <sub>2</sub> O <sub>3</sub>	3.11	7.61	3.28	3.36	5.71	3.04	3.06	3.76
Tb <sub>2</sub> O <sub>3</sub>	0.39	0.61	0.26	0.30	0.38	0.28	0.26	0.19
Dy <sub>2</sub> O <sub>3</sub>	1.34	1.50	0.83	0.66	0.78	0.87	0.74	0.35
Ho <sub>2</sub> O <sub>3</sub>	0.15	0.11	0.07	0.04	0.00	0.04	0.00	0.00
Er <sub>2</sub> O <sub>3</sub>	0.50	0.29	0.28	0.30	0.25	0.35	0.31	0.26
Tm <sub>2</sub> O <sub>3</sub>	0.11	0.09	0.05	0.12	0.10	0.08	0.07	0.09
Yb <sub>2</sub> O <sub>3</sub>	0.62	0.12	0.14	0.14	0.15	0.11	0.13	0.16
Lu <sub>2</sub> O <sub>3</sub>	0.06	0.06	0.08	0.09	0.07	0.05	0.11	0.08
FeO	0.00	0.00	0.78	0.00	0.00	0.00	0.00	0.00
CaO	1.86	0.67	1.46	2.54	0.96	1.73	2.09	1.02
PbO	0.01	0.00	0.01	0.01	0.00	0.02	0.02	0.01
<b>Total</b>	100.96	99.47	99.82	101.08	100.08	99.76	99.84	98.92
Formulae based on 4 oxygen atoms								
P	0.965	0.986	0.962	0.971	0.988	0.955	0.967	0.976
As	0.002	0.002	0.002	0.002	0.002	0.005	0.005	0.005
Si	0.025	0.009	0.020	0.017	0.012	0.030	0.016	0.014
<b>Sum B</b>	0.992	0.997	0.985	0.990	1.002	0.991	0.987	0.995
Th	0.067	0.018	0.067	0.098	0.034	0.086	0.048	0.037
U	0.024	0.015	0.009	0.022	0.010	0.010	0.044	0.011
Y	0.096	0.064	0.045	0.029	0.032	0.045	0.038	0.011
La	0.133	0.081	0.145	0.137	0.111	0.140	0.145	0.141
Ce	0.302	0.270	0.338	0.316	0.312	0.333	0.339	0.356
Pr	0.039	0.045	0.045	0.040	0.046	0.044	0.044	0.050
Nd	0.146	0.215	0.166	0.136	0.203	0.159	0.150	0.195
Sm	0.053	0.134	0.067	0.066	0.114	0.063	0.066	0.101
Eu	0.000	0.000	0.001	0.000	0.000	0.000	0.000	0.000
Gd	0.040	0.100	0.043	0.044	0.075	0.040	0.040	0.050
Tb	0.005	0.008	0.003	0.004	0.005	0.004	0.003	0.002
Dy	0.017	0.019	0.011	0.008	0.010	0.011	0.010	0.005
Ho	0.002	0.001	0.001	0.001	0.000	0.000	0.000	0.000
Er	0.006	0.004	0.004	0.004	0.003	0.004	0.004	0.003
Tm	0.001	0.001	0.001	0.002	0.001	0.001	0.001	0.001
Yb	0.007	0.001	0.002	0.002	0.002	0.001	0.002	0.002
Lu	0.001	0.001	0.001	0.001	0.001	0.001	0.001	0.001
Fe	0.000	0.000	0.026	0.000	0.000	0.000	0.000	0.000
Ca	0.077	0.028	0.062	0.107	0.041	0.074	0.089	0.044
Pb	0.000	0.000	0.000	0.000	0.000	0.000	0.000	0.000
<b>Sum A</b>	1.017	1.006	1.035	1.016	0.999	1.017	1.024	1.008
La/Nd	0.91	0.38	0.87	1.00	0.55	0.88	0.96	0.72
La/Sm	2.52	0.60	2.17	2.07	0.97	2.22	2.20	1.40
La/Gd	3.32	0.81	3.34	3.12	1.48	3.50	3.59	2.81

S, Al, Sr below detection limit.

important role of magmatic fractional crystallization during monazite growth and effective separation from feldspar-rich, residual magma probably of granitic composition, where Eu in divalent form is preferentially bounded in feldspars, especially Ca-bearing plagioclase. Strong negative Eu-anomaly ( $\text{Eu}/\text{Eu}^* \sim 10^{-2}$  magnitude) is a characteristic feature of granitic rocks that originated from melting of crustal rocks (Bea 1996). Moreover, distinct variations in La/Nd, La/Sm, La/Gd, and La/Y ratios also document an effective fractionation of REEs during monazite precipitation.

*Uraninite* is a relatively widespread accessory mineral in peraluminous leucogranites as well as abyssal to rare-element granitic pegmatites (e.g. Bea 1996; Černý & Ercit 2005; McKechnie et al. 2012). The Visole pegmatite contains euhedral uraninite inclusions in albite and spessartine-almandine and minute anhedral inclusions in zircon from this pegmatite. The euhedral uraninite shows Th-rich compositions (2.5 to 3.7 wt. % ThO<sub>2</sub>), which are a characteristic feature of magmatic uraninite (usually with 1 to 20 wt. % ThO<sub>2</sub>; Bea 1996; Finch & Mukarami 1999; Förster 1999; Hazen et al. 2009; Petrík & Konečný 2009), in contrast to Th-poor uraninite (usually <0.5 wt. % ThO<sub>2</sub>) from hydrothermal and sedimentary occurrences (e.g. Alexandre & Kyser 2005; Deditius et al. 2007). Analogous primary magmatic inclusions of uraninite in garnet have been locally described from peraluminous granites (Petrík & Konečný 2009) and granitic pegmatites (Sen et al. 2009; Lima et al. 2012). On the contrary, the anhedral uraninite inclusions in zircon are probably products of subsolidus degradation of the metamict host mineral.

#### Age of the pegmatite

Both monazite and uraninite show Miocene ages between ca. 20 and 14 Ma. Our results of monazite chemical dating ( $17.2 \pm 1.8$  Ma) are consistent with LA ICP-MS dating of zircon in tonalite from the eastern part of the Pohorje pluton with a concordant age of  $18.6 \pm 0.1$  Ma (Fodor et al. 2008), and K-Ar ages ( $20.3 \pm 1.1$  Ma to  $14.9 \pm 0.6$  Ma; Fodor et al. 2008; Trajanova et al. 2008) of biotite, amphibole and feldspar from gabbros, tonalites, granodiorites, granitic porphyries and volcanic rocks (mainly dacites) of the Pohorje Mountains. The younger age of the uraninite (~14 Ma) is probably due to episodic partial loss of Pb. Therefore, age dating of the Visole pegmatite reveals its origin during the Miocene calc-alkaline plutonic-volcanic activity.

Our dating results represent the first direct evidence of Neogene granitic pegmatites in the Pohorje Mountains as well as in broader area of the Eastern Alps. Populations of Alpine, Paleogene to Neogene granitic pegmatites are relatively scarce in Europe, in comparison to the Paleozoic and Precambrian pegmatite fields. They are concentrated only along the young Alpine-orogen related, post-collisional fault

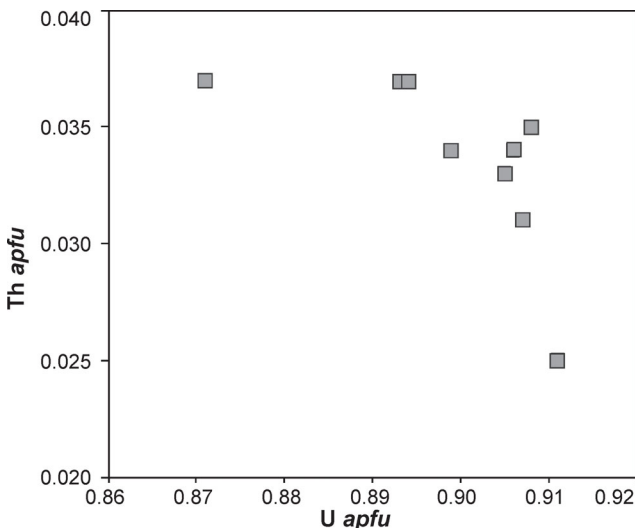


**Fig. 7.** Th vs. U substitution diagram of uraninite from the Visole pegmatite (atomic proportions).

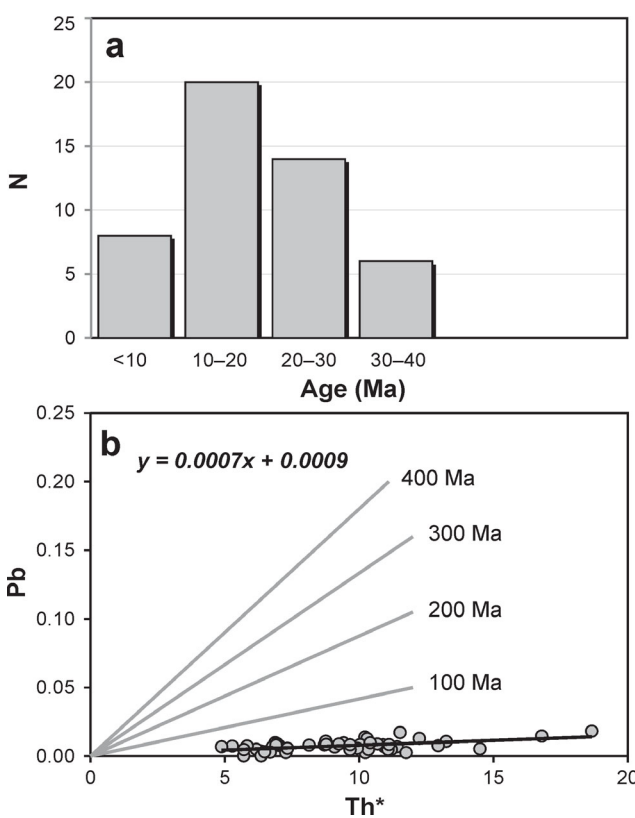


**Fig. 8.** Monazite chemical dating from the Visole pegmatite. **a** — Age histogram (Ma); **b** — Pb vs. Th\* diagram (wt. %).  $\text{Th}^* = \text{Th} + 3.15\text{U}$  (wt. %).

zones between the continental fragments, such as the Periadriatic, Aegean, and Corsica-Apulia zones.

A province of Oligocene granitic pegmatites, locally containing rare-element mineralization with beryl, columbite, euxenite, vigezzite and other Nb-Ta-(Ti-Y-REE) phases, galolinite, schorl-elbaite, monazite, xenotime, etc., occurs to-

**Table 6:** Representative compositions of uraninite (wt. %) from the Visole pegmatite.

Position/Anal.	in Ab/1	in Gar/2	in Gar/3	in Gar/4
$\text{As}_2\text{O}_5$	0.19	0.15	0.18	0.16
$\text{SiO}_2$	0.08	0.07	0.10	0.26
$\text{ThO}_2$	3.00	3.20	2.45	3.66
$\text{UO}_2$	90.65	90.24	90.98	88.90
$\text{Y}_2\text{O}_3$	0.97	0.51	0.42	0.56
$\text{Ce}_2\text{O}_3$	0.20	0.17	0.14	0.19
$\text{Pr}_2\text{O}_3$	0.36	0.30	0.37	0.36
$\text{Nd}_2\text{O}_3$	0.04	0.08	0.08	0.09
$\text{Sm}_2\text{O}_3$	0.40	0.32	0.24	0.33
$\text{Eu}_2\text{O}_3$	0.23	0.19	0.31	0.32
$\text{Gd}_2\text{O}_3$	0.36	0.27	0.20	0.27
$\text{Tb}_2\text{O}_3$	0.14	0.14	0.19	0.11
$\text{Dy}_2\text{O}_3$	0.38	0.19	0.16	0.19
$\text{Er}_2\text{O}_3$	0.54	0.49	0.48	0.49
$\text{Tm}_2\text{O}_3$	0.12	0.11	0.12	0.12
$\text{Yb}_2\text{O}_3$	0.20	0.21	0.17	0.16
$\text{Lu}_2\text{O}_3$	0.11	0.12	0.15	0.05
$\text{FeO}$	0.00	0.81	0.86	1.92
$\text{PbO}$	0.17	0.17	0.17	0.16
<b>Total</b>	98.14	97.74	97.77	98.30

Formulae based on 2 oxygen atoms

As	0.004	0.004	0.004	0.004
Si	0.004	0.003	0.005	0.011
Th	0.031	0.033	0.025	0.037
U	0.907	0.905	0.911	0.871
Y	0.023	0.012	0.010	0.013
Ce	0.003	0.003	0.002	0.003
Pr	0.006	0.005	0.006	0.006
Nd	0.001	0.001	0.001	0.001
Sm	0.006	0.005	0.004	0.005
Eu	0.004	0.003	0.005	0.005
Gd	0.005	0.004	0.003	0.004
Tb	0.002	0.002	0.003	0.002
Dy	0.006	0.003	0.002	0.003
Er	0.008	0.007	0.007	0.007
Tm	0.002	0.002	0.002	0.002
Yb	0.003	0.003	0.002	0.002
Lu	0.001	0.002	0.002	0.001
Fe	0.000	0.031	0.032	0.071
Pb	0.002	0.002	0.002	0.002
<b>Sum cat.</b>	1.017	1.028	1.028	1.049
<b>U/Th</b>	29.3	27.4	36.4	23.5

S, P, Al, La, Ho, Ca, Sr below detection limit.

gether with Paleogene granitic rocks along the Periadriatic (Insubric) line in the Central and Western Alps (e.g. Wenger & Armbruster 1991; Aurisicchio et al. 2001; Guastoni et al. 2008; Guastoni 2012). The radiometric age of the pegmatite crystallization along the Insubric line (Isorno-Orselina and Monte Rosa zones) was determined by the isotopic U-Pb method on monazite and xenotime in the interval of 29 to 25 Ma, whereas the Rb-Sr as well as Ar-Ar muscovite and biotite dating yielded cooling ages of 25 to 19 Ma (Schärer et al. 1996). Analogous isotopic U-Pb results on monazite, xenotime and zircon ( $29.2 \pm 0.2$  Ma) were obtained from aplites and pegmatites along the Centovalli line, Italy (Romer et al. 1996). A slightly older age of  $32.7 \pm 3.2$  Ma has been obtained by total U-Th-Pb m-PIXE method on cheralite from the beryl (emerald) and Nb-minerals bearing pegmatites of the Vigezzo Valley, Italy (Guastoni & Mazzoli 2007).

Intrusions of late Cretaceous, Paleogene to early Miocene granitic rocks and related pegmatites are widespread in the

Rhodope Massif of the Aegean Zone, Greece and Bulgaria (e.g. Kilias & Mountrakis 1998; Soldatos et al. 2008; Pipera et al. 2013). Locally, Paleogene rare-element granitic pegmatites with beryl (emerald) and columbite-group minerals were described, for example, the Rila emerald-bearing peg-

matite in Bulgaria shows Late Eocene Ar-Ar phlogopite age of  $34.2 \pm 0.4$  Ma (Alexandrov et al. 2001).

On the other hand, Late Miocene to Pliocene pegmatites are associated with granitic rocks in the Tuscany magmatic province, mainly in the Monte Capanne pluton of the Island

**Table 7:** Measured and corrected element concentrations and chemical ages of monazite and uraninite calculated by Montel et al. (1996).

Sample/ Crystal/Point	Th wt. %	U wt. %	Pb wt. %	Y wt. %	Ucor wt. %	Pbcor wt. %	Th 2σ	U 2σ	Pb 2σ	Age (Ma)	± Ma (1σ)
<b>Monazite</b>											
Vi-11A/Mnz1/1	6.6584	2.5440	0.0518	3.6545	2.4668	0.0053	0.0368	0.0217	0.0055	8.3	9.5
Vi-11A/Mnz1/2	6.8724	2.0823	0.0467	2.6343	2.0026	0.0108	0.0373	0.0197	0.0055	18.5	9.5
Vi-11A/Mnz1/3	6.5002	1.7280	0.0354	2.3948	1.6526	0.0026	0.0363	0.0182	0.0055	5.0	8.8
Vi-11A/Mnz2/1	1.6698	1.0291	0.0277	2.0326	1.0097	0.0069	0.0211	0.0152	0.0055	32.1	25.8
Vi-11A/Mnz2/2	1.7163	1.4795	0.0250	2.3883	1.4596	0.0003	0.0213	0.0170	0.0055	0.9	11.3
Vi-11A/Mnz2/3	1.6705	1.7814	0.0339	3.0169	1.7620	0.0025	0.0211	0.0183	0.0055	7.9	13.6
Vi-11A/Mnz2/4	3.7126	0.6706	0.0182	1.0190	0.6275	0.0048	0.0283	0.0137	0.0054	19.0	21.4
Vi-11A/Mnz2/5	3.3254	1.0960	0.0211	1.5267	1.0574	0.0029	0.0271	0.0155	0.0054	9.8	15.2
Vi-11A/Mnz2/6	3.3736	1.0167	0.0177	1.1831	0.9776	0.0031	0.0273	0.0152	0.0055	10.8	16.1
Vi-11A/Mnz3/1	6.5312	0.9852	0.0347	1.6657	0.9094	0.0097	0.0364	0.0150	0.0054	23.3	13.1
Vi-11A/Mnz4/1	7.0708	1.3520	0.0397	2.1618	1.2700	0.0085	0.0377	0.0165	0.0054	17.3	11.1
Vi-11A/Mnz4/2	6.9462	1.1500	0.0304	1.6406	1.0694	0.0049	0.0374	0.0157	0.0054	10.8	12.4
Vi-11A/Mnz4/3	6.7646	1.0736	0.0305	1.6057	0.9951	0.0057	0.0371	0.0155	0.0055	13.1	12.6
Vi-11A/Mnz4/4	5.6341	1.0319	0.0196	0.5416	0.9665	0.0081	0.0339	0.0152	0.0054	21.1	14.2
Vi-11A/Mnz4/5	7.8113	0.9915	0.0361	1.6655	0.9009	0.0090	0.0395	0.0150	0.0055	19.0	11.7
Vi-11A/Mnz4/6	6.2849	1.1357	0.0228	0.7206	1.0628	0.0083	0.0357	0.0157	0.0054	19.5	12.8
Vi-11A/Mnz5/1	5.9603	1.1018	0.0202	0.4710	1.0327	0.0089	0.0349	0.0157	0.0054	21.9	13.4
Vi-11A/Mnz5/2	5.6102	1.0531	0.0231	0.6103	0.9880	0.0110	0.0338	0.0153	0.0054	28.3	14.2
Vi-11A/Mnz5/3	9.6117	2.3708	0.0388	1.1099	2.2593	0.0147	0.0439	0.0209	0.0055	19.7	7.5
Vi-11A/Mnz5/4	5.8688	1.4954	0.0249	0.8494	1.4273	0.0098	0.0345	0.0171	0.0054	21.2	11.9
Vi-11A/Mnz5/5	5.8267	1.2753	0.0185	0.7184	1.2077	0.0048	0.0344	0.0163	0.0054	11.2	13.0
Vi-11A/Mnz5/6	9.0976	1.3160	0.0280	0.8394	1.2105	0.0075	0.0426	0.0165	0.0055	13.2	9.6
Vi-11A/Mnz5/7	4.1892	1.0355	0.0164	0.6877	0.9869	0.0058	0.0298	0.0153	0.0055	17.8	17.1
Vi-11A/Mnz5/8	5.4729	1.0999	0.0206	0.6083	1.0364	0.0087	0.0335	0.0155	0.0054	22.4	14.1
Vi-11B/Mnz1/1	2.9026	1.1188	0.0245	1.8491	1.0851	0.0036	0.0257	0.0155	0.0054	12.7	17.2
Vi-11B/Mnz1/2	2.7429	1.1113	0.0282	2.0800	1.0795	0.0051	0.0250	0.0155	0.0055	18.6	20.6
Vi-11B/Mnz1/3	2.7640	0.9572	0.0182	1.5828	0.9251	0.0003	0.0251	0.0148	0.0054	1.3	12.5
Vi-11B/Mnz2/1	8.2279	1.0965	0.0354	1.7301	1.0011	0.0069	0.0405	0.0155	0.0054	13.6	10.8
Vi-11B/Mnz2/2	7.1601	1.2694	0.0347	1.8262	1.1863	0.0069	0.0379	0.0162	0.0054	14.3	11.3
Vi-11B/Mnz2/3	6.6512	1.2046	0.0332	2.1661	1.1274	0.0026	0.0366	0.0159	0.0054	5.7	9.9
Vi-11B/Mnz2/4	7.2051	1.0285	0.0409	1.7515	0.9449	0.0139	0.0379	0.0152	0.0054	30.8	12.2
Vi-11B/Mnz2/5	7.8887	1.1306	0.0331	1.7451	1.0391	0.0050	0.0397	0.0157	0.0054	10.0	11.5
Vi-11B/Mnz2/6	7.6380	1.1106	0.0358	1.7208	1.0220	0.0084	0.0391	0.0155	0.0054	17.4	11.3
Vi-11B/Mnz2/7	5.8890	1.0730	0.0324	1.8447	1.0047	0.0065	0.0345	0.0153	0.0054	16.3	13.6
Vi-11B/Mnz2/8	6.6579	1.2211	0.0426	2.1020	1.1439	0.0128	0.0367	0.0160	0.0054	28.0	12.0
Vi-11B/Mnz2/9	8.3723	1.0869	0.0451	1.6589	0.9898	0.0172	0.0409	0.0155	0.0054	33.7	10.8
Vi-11B/Mnz2/10	8.0745	1.0380	0.0322	1.6432	0.9443	0.0048	0.0402	0.0153	0.0054	9.9	11.5
Vi-11B/Mnz3/1	3.6593	2.7400	0.0293	1.3115	2.6976	0.0129	0.0281	0.0224	0.0054	24.0	10.2
Vi-11B/Mnz3/2	4.6382	4.4625	0.0371	1.3971	4.4087	0.0182	0.0309	0.0300	0.0054	22.2	6.7
Vi-11B/Mnz4/1	3.1304	0.7112	0.0165	0.7230	0.6749	0.0073	0.0264	0.0139	0.0054	31.1	23.5
Vi-11B/Mnz4/2	5.7897	0.8042	0.0177	0.3437	0.7370	0.0081	0.0343	0.0143	0.0053	22.4	15.0
Vi-11B/Mnz4/3	4.8698	0.7331	0.0226	0.9735	0.6766	0.0078	0.0317	0.0139	0.0053	25.0	17.4
Vi-11B/Mnz4/4	4.6832	0.7439	0.0191	0.4822	0.6896	0.0099	0.0312	0.0140	0.0053	32.4	17.8
Vi-11B/Mnz4/5	6.6620	1.1383	0.0295	1.2761	1.0610	0.0085	0.0367	0.0156	0.0054	19.0	12.3
Vi-11B/Mnz4/6	3.5614	0.7548	0.0161	0.5947	0.7135	0.0075	0.0279	0.0141	0.0054	29.2	21.3
Vi-11BMnz5/1	3.5501	1.1065	0.0156	0.3896	1.0653	0.0092	0.0277	0.0154	0.0053	30.2	17.7
Vi-11B/Mnz5/2	4.0571	0.8995	0.0173	0.6979	0.8524	0.0068	0.0293	0.0146	0.0054	22.7	18.3
Vi-11B/Mnz5/3	3.8955	0.9903	0.0155	0.4369	0.9451	0.0081	0.0288	0.0149	0.0054	26.4	18.0
<b>Uraninite</b>											
Vi-11B/Urn1/1	2.6395	79.9392	0.1683	0.7606	79.9086	0.1610	0.0236	0.3997	0.0061	14.3	0.6
Vi-11B/Urn1/2	2.9394	79.5689	0.1681	0.7525	79.5348	0.1604	0.0245	0.3979	0.0061	14.3	0.6
Vi-11B/Urn1/3	2.9768	79.4774	0.1694	0.7124	79.4429	0.1621	0.0247	0.3975	0.0061	14.4	0.6
Vi-11B/Urn2/1	3.1819	79.3887	0.1607	0.4202	79.3518	0.1561	0.0253	0.3971	0.0061	13.9	0.6
Vi-11B/Urn2/2	2.8147	79.5823	0.1628	0.4018	79.5496	0.1590	0.0242	0.3980	0.0061	14.2	0.6
Vi-11B/Urn2/3	2.1510	80.2243	0.1654	0.3293	80.1993	0.1636	0.0220	0.4011	0.0061	14.5	0.6
Vi-11B/Urn2/4	3.1790	78.7474	0.1635	0.4128	78.7105	0.1590	0.0253	0.3939	0.0061	14.3	0.6
Vi-11B/Urn2/5	2.8960	79.0024	0.1612	0.4096	78.9688	0.1572	0.0244	0.3951	0.0061	14.1	0.6
Vi-11B/Urn2/6	3.2168	78.4043	0.1586	0.4401	78.3670	0.1537	0.0254	0.3922	0.0061	13.9	0.6

of Elba. Rare-element granitic pegmatites with Li-bearing tourmalines (schorl to fluorelbaite) and Nb-Ta oxide minerals (mainly members of columbite and euxenite group minerals) form dikes and fillings of miarolitic vugs in parental monzogranites (Pezzotta 2000; Aurisicchio et al. 2002; Guastoni et al. 2008; Guastoni 2012). The granitic rocks and related pegmatite dikes of the island of Elba were emplaced during the Late Miocene (Tortonian to Messinian), ~8 to 6.7 Ma ago, as determined by the Rb-Sr and Nd whole-rock and mineral-rock isochron dating (Ferrara & Tonarini 1985; Dini et al. 2002, and references therein). Similar pegmatite and aplite dykes cut monzogranites in the adjacent plutons of Montecristo (7.1 Ma; Innocenti et al. 1997) and Giglio islands (~5 Ma; Peccerillo 2005). However, the youngest plutonic activity of the Tuscany magmatic province terminated during the Pliocene at 4.5 to 4.3 Ma ago, while volcanism of the Roman and Tuscan provinces has been active up to the Quaternary (Dini et al. 2002; Peccerillo 2005).

#### Pegmatite source and evolution

The mineralogical character of the Visole pegmatite, rich in Al-rich silicate minerals (muscovite, spessartine-almandine), indicate its origin from a peraluminous magma source. The Miocene age of the Visole pegmatite is consistent with the adjacent Pohorje pluton. Consequently, a direct origin of such magma by fractionation of the Pohorje calc-alkaline granodiorites-tonalites is not probable. However, we can assume the formation of small leucogranitic stocks which possibly originated by partial anatexis of a peraluminous metapelitic protolith due to intrusion of the Pohorje pluton. Metapelitic rocks (gneisses, micaschists) overprinted by Cretaceous HP-UHP metamorphism are widespread lithologies around the Pohorje pluton (e.g. Janák et al. 2004, 2009; Krenn et al. 2009; Kirst et al. 2010). Successive fractionation of the leucogranite magma from these satellite bodies around the Pohorje pluton resulted in formation of the pegmatite melt which escaped and intruded into the host metamorphic rocks. Such a petrogenetic scenario corresponds to recent knowledge concerning the origin of evolved granitic pegmatites with rare-element specialization (London 2008 and references therein).

An application of the monazite-garnet geothermometry (Pyle et al. 2001) indicates a temperature of  $\sim 495 \pm 30$  °C (at estimated 4 to 5 kbar pressure) for precipitation of the monazite-garnet-apatite-plagioclase assemblage. Such temperatures are common for the solidification of evolved pegmatite magma (London 2008 and references therein). However, the geothermometer was calibrated for the mineral equilibrium in metamorphic rocks (metapelites) and the resulting temperatures represent only approximate values.

#### Conclusions

The Miocene granitic pegmatite intruding UHP metamorphic rocks at Visole in the Pohorje Mts, shows a muscovite — rare-element, or rare-element, beryl-columbite and LCT geochemical affinity (sensu Černý & Ercit 2005). Chemical dating of monazite and uraninite (~17 to 14 Ma) clearly re-

veals the Miocene age of the pegmatite, the emplacement and solidification of which was coeval with the calc-alkaline plutonic and volcanic activity in the Pohorje Mountains. The Visole pegmatite represents the first documented example of rare-element granitic pegmatite of Miocene age in the Eastern Alps and it belongs to the youngest populations of granitic pegmatites in Europe. It is younger than Paleogene pegmatite populations in the Rhodope Massif and along the Periadriatic (Insubric) line but older than the Late Miocene to Pliocene pegmatites of the Tuscany magmatic province.

The apparently negative Eu-anomaly of monazite and the composition of minerals document an important role of magmatic fractionation from a parental granitic source. However, the pegmatite did not originate directly from the adjacent tonalitic-granodioritic rocks of the Pohorje pluton. The pegmatite magma was probably generated by magmatic fractionation of possible small satellite leucogranitic stocks around the Pohorje pluton. They originated from partial anatexis of a peraluminous metapelitic source during emplacement of the Pohorje tonalite-granodiorite pluton.

**Acknowledgments:** The authors thank A. Guastoni, R. Škoda and I. Petrik for constructive criticism and suggestions that improved the manuscript. The paper has also benefitted from discussion with M. Kováč. This work was financially supported by the Slovak Research and Development Agency under the contract Nos. APVV-0080-11, APVV-0557-06, and APVV-VVCE-0033-07 SOLIPHA, and the Slovak Scientific Grant Agency VEGA (Grant No. 2/0013/12).

#### References

- Alexandre P. & Kyser T.K. 2005: Effects of cationic substitutions and alteration in uraninite, and implications for the dating of uranium deposits. *Canad. Mineralogist* 43, 1005–1017.
- Alexandrov P., Giuliani G. & Zimmermann J.L. 2001: Mineralogy, age, and fluid geochemistry of the Rila emerald deposit, Bulgaria. *Econ. Geol.* 96, 1469–1476.
- Altherr R., Lugovic B., Meyer H.P. & Majer V. 1995: Early Miocene post-collisional calc-alkaline magmatism along the easternmost segment of the periadiatic fault system (Slovenia and Croatia). *Miner. Petrology* 54, 225–247.
- Aurisicchio C., De Vito C., Ferrini V. & Orlandi P. 2001: Nb-Ta oxide minerals from miarolitic pegmatites of the Baveno pink granite, NW Italy. *Mineral. Mag.* 65, 509–522.
- Aurisicchio C., De Vito C., Ferrini V. & Orlandi P. 2002: Nb and ta oxide minerals in the Fonte del Prete granitic pegmatite dike, Island of Elba, Italy. *Canad. Mineralogist* 40, 799–814.
- Baldwin J.R. & von Knorring O. 1983: Compositional range of Mn-garnet in zoned granitic pegmatites. *Canad. Mineralogist* 21, 683–688.
- Bea F. 1996: Residence of REE, Y, Th and U in granites and crustal protoliths; implications for the chemistry of crustal melts. *J. Petrology* 37, 521–552.
- Benedek K., Pécskay Z., Szabó Cs., Jósavai J. & Németh T. 2004: Paleogene igneous rocks in the Zala Basin (Western Hungary): Link to the Palaeogene magmatic activity along the Periadriatic Lineament. *Geol. Carpathica* 55, 43–50.
- Bowles J.F.W. 1990: Age dating of individual grains of uraninite in rocks from electron microprobe analyses. *Chem. Geol.* 83, 47–53.

- Breiter K. & Škoda R. 2012: Vertical zonality of fractionated granite plutons reflected in zircon chemistry: the Cínovec A-type versus the Beauvoir S-type suite. *Geol. Carpathica* 63, 383–398.
- Breiter K., Förster H.-J. & Škoda R. 2006: Extreme P-, Bi-, Nb-, Sc-, U- and F-rich zircon from fractionated perphosphorous granites: The peraluminous Podlesí granite system, Czech Republic. *Lithos* 88, 15–34.
- Cameron-Schiman M. 1978: Electron microprobe study of uranium minerals and its application to some Canadian deposits. *Ph.D. Thesis, University of Alberta*, Edmonton, Alberta, 1–343 (unpublished).
- Černý P. 1989: Characteristics of pegmatite deposits of tantalum. In: Möller P., Černý P. & Saupé F. (Eds.): Lanthanides, Tantalum and Niobium. *Springer-Verlag*, Berlin, 195–239.
- Černý P. & Ercit T.S. 2005: The classification of granitic pegmatites revisited. *Canad. Mineralogist* 43, 2005–2026.
- Černý P., Meintzer R.E. & Anderson A.J. 1985: Extreme fractionation in rare-element granitic pegmatites: selected examples of data and mechanisms. *Canad. Mineralogist* 23, 381–421.
- Černý P., Goad B.E., Hawthorne F.C. & Chapman R. 1986: Fractionation trends of the Nb- and Ta-bearing oxide minerals in the Greer Lake pegmatitic granite and its pegmatitic aureole, southeastern Manitoba. *Amer. Mineralogist* 71, 501–517.
- Černý P., Teertstra D., Chapman R., Selway J., Hawthorne F.C., Ferreira K., Chackowsky L.E., Wang X.-J. & Meitzer R.E. 2012: Extreme fractionation and deformation of the leucogranite-pegmatite suite at Red Cross Lake, Manitoba, Canada. IV. Mineralogy. *Canad. Mineralogist* 50, 1839–1875.
- Chudík P., Uher P., Gadas P., Škoda R. & Pršek J. 2011: Niobium-tantalum oxide minerals in the Jezuitské Lesy granitic pegmatite, Bratislava Massif, Slovakia: Ta to Nb and Fe to Mn evolutionary trends in a narrow Be,Cs-rich and Li,B-poor dike. *Miner. Petrology* 102, 15–27.
- Deditius A.P., Utsunomiya S. & Ewing R.C. 2007: Fate of trace elements during alteration of uraninite in a hydrothermal vein-type U-deposit from Marshall Pass, Colorado, USA. *Geochim. Cosmochim. Acta* 71, 4954–4973.
- De Hoog J.C.M., Janák M., Vrabec M. & Froitzheim N. 2009: Serpentised peridotites from an ultra-high pressure terrane in the Pohorje Mts. (Eastern Alps, Slovenia): Geochemical constraints on petrogenesis and tectonic setting. *Lithos* 109, 209–222.
- De Hoog J.C.M., Janák M., Vrabec M. & Hattori K.H. 2011: Ultramafic cumulates of oceanic affinity in an intracontinental subduction zone: ultrahigh-pressure garnet peridotites from Pohorje (Eastern Alps, Slovenia). In: Dobrzhinetskaya L.F., Faryad S.W., Wallis S. & Cuthbert S. (Eds.): Ultra-high pressure metamorphism, 25 years after the discovery of coesite and diamond. *Elsevier*, Amsterdam, 399–439.
- Dini A., Innocenti F., Rocchi S., Tonarini S. & Westerman D.S. 2002: The magmatic evolution of the late Miocene laccolith-pluton-dyke granitic complex of Elba Island, Italy. *Geol. Mag.* 139, 257–279.
- Ferrara G. & Tonarini S. 1985: Radiometric geochronology in Tuscany: results and problems. *Rend. Soc. Ital. Miner. Petrology* 40, 111–124.
- Finch R.J. & Murakami T. 1999: Systematics and paragenesis of uranium minerals. In: Burns P.C. & Finch R. (Eds.): Uranium: Mineralogy, geochemistry and the environment. *Rev. Mineral. Geochem.* 38; *Mineral. Soc. Amer.*, Chantilly, Virginia, 91–180.
- Fodor L.I., Gerdes A., Dunkl I., Koroknai B., Pécsay Z., Trajanova M., Horváth P., Vrabec M., Jelen B., Balogh K. & Frisch W. 2008: Miocene emplacement and rapid cooling of the Pohorje pluton at the Alpine-Pannonian-Dinaric junction, Slovenia. *Swiss J. Geosci.* 101, Suppl. 1, S255–S271.
- Förster H.-J. 1999: The chemical composition of uraninite in Variscan granites of the Erzgebirge, Germany. *Mineral. Mag.* 63, 239–252.
- Gbelšký J. 1980: Composition of the main morphological types of garnets from pegmatites of the Malé Karpaty Mts (the West Carpathians). *Geol. Zbor. Geol. Carpath.* 30, 463–474.
- Guastoni A. 2012: LCT (lithium, cesium, tantalum) and NYF (niobium, yttrium, fluorine) pegmatites in the Central Alps, Proxies of exhumation history of the Alpine stack in the Lepontine Dome. *Unpubl. PhD. Thesis, Univ. Padova*, 1–189.
- Guastoni A. & Mazzoli C. 2007: Age determination by  $\mu$ -PIXE analysis of cheralite-(Ce) from emerald-bearing pegmatites of Vigezzo Valley (Western Alps, Italy). *Mitt. Österr. Mineral. Gesell.* 153, 279–282.
- Guastoni A., Diela V. & Pezzotta F. 2008: Vigezzite and associated oxides of Nb-Ta from emerald-bearing pegmatites of the Vigezzo Valley, Western Alps, Italy. *Canad. Mineralogist* 46, 619–633.
- Hazen R.M., Ewing R.C. & Sverjensky D.A. 2009: Evolution of uranium and thorium minerals. *Amer. Mineralogist* 94, 1293–1311.
- Hinterlechner-Ravnik A., Sassi F.P. & Visona D. 1991: The Austrodiac eclogites, metabasites and metaultabasites from the Pohorje area (Eastern Alps, Yugoslavia). 2. The metabasites and metaultabasites, and concluding considerations. *Rendic. Fisiche Accad. Lincei* 2, 175–190.
- Hoinkes G., Koller F., Rantisch G., Dachs E., Höck V., Neubauer F. & Schuster R. 1999: Alpine metamorphism of the Eastern Alps. *Schweiz. Mineral. Petrogr. Mitt.* 79, 155–181.
- Holland T.J.B. & Powell R. 1998: An internally consistent thermodynamic data set for phases of petrological interest. *J. Metamorph. Geology* 16, 309–343.
- Innocenti F., Westerman D.S., Rocchi S. & Tonarini S. 1997: The Montecristo monzogranite (Northern Tyrrhenian Sea, Italy): a collisional pluton in an extensional setting. *Geol. J.* 32, 131–151.
- Janák M., Froitzheim N., Lupták B., Vrabec M. & Krogh Ravna E.J. 2004: First evidence for ultrahigh-pressure metamorphism of eclogites in Pohorje, Slovenia: Tracing deep continental subduction in the Eastern Alps. *Tectonics* 23, TC5014. Doi:10.1029/2004TC001641
- Janák M., Froitzheim N., Vrabec M., Krogh Ravna E.J. & De Hoog J.C.M. 2006: Ultrahigh-pressure metamorphism and exhumation of garnet peridotite in Pohorje, Eastern Alps. *J. Metamorph. Geology* 24, 19–31.
- Janák M., Cornell D., Froitzheim N., De Hoog J.C.M., Broska I., Vrabec M. & Hurai V. 2009: Eclogite-hosting metapelites from the Pohorje Mountains (Eastern Alps): P-T evolution, zircon geochronology and tectonic implications. *Eur. J. Mineral.* 21, 1191–1212.
- Kiliás A.A. & Mountrakis D.M. 1998: Tertiary extension of the Rhodope massif associated with granite emplacement. (Northern Greece). *Acta Vulcanol.* 10, 331–337.
- Kirst F., Sandmann S., Nagel T.J., Froitzheim N. & Janák M. 2010: Tectonic evolution of the southeastern part of the Pohorje Mountains (Eastern Alps, Slovenia). *Geol. Carpathica* 61, 451–461.
- Konečný P., Siman P., Holický I., Janák M. & Kollárová V. 2004: Methodics of monazite dating using an electron microprobe. *Miner. Slovaca* 36, 225–235 (in Slovak with English summary).
- Kovács I., Csontos L., Szabó Cs., Bali E., Falus Gy., Benedek K. & Zajacz Z. 2007: Paleogene-early Miocene igneous rocks and geodynamics of the Alpine-Carpathian-Pannonian-Dinaric region: An integrated approach. *Geol. Soc. Amer., Spec. Pap.* 418, 93–112.
- Krenn E., Janák M., Finger F., Broska I. & Konečný P. 2009: Two types of metamorphic monazite with contrasting La/Nd, Th,

- and Y signatures in an ultrahigh-pressure metapelite from the Pohorje Mountains, Slovenia: Indications for pressure-dependent REE exchange between apatite and monazite? *Amer. Mineralogist* 94, 801–815.
- Lima S.M., Corfu F., Neiva A.M.R. & Ramos J.M.F. 2012: U-Pb ID-TIMS dating applied to U-rich inclusions in garnet. *Amer. Mineralogist* 97, 800–806.
- London D. 2008: Pegmatites. *Canad. Mineralogist, Spec. Publ.* 10, 1–348.
- Lustrino M., Duggen S. & Rosenberg C.L. 2011: The Central-Western Mediterranean: Anomalous igneous activity in an anomalous collisional tectonic setting. *Earth Sci. Rev.* 104, 1–40.
- Márton E., Trajanova M., Zupančič N. & Jelen B. 2006: Formation, uplift and tectonic integration of a Periadriatic intrusive complex (Pohorje, Slovenia) as reflected in magnetic parameters and palaeomagnetic directions. *Geophys. J. Int.* 167, 1148–1159.
- McKechnie C., Annesley I.R. & Ansdell K.M. 2012: Radioactive abyssal granitic pegmatites and leucogranites in the Wollaston Domain, northern Saskatchewan, Canada: mineral compositions and conditions of emplacement on the Fraser Lakes area. *Canad. Mineralogist* 50, 1637–1667.
- Miller C., Mundil R., Thöni M. & Konzett J. 2005: Refining the timing of eclogite metamorphism: a geochemical, petrological, Sm-Nd and U-Pb case study from the Pohorje Mountains, Slovenia (Eastern Alps). *Contr. Mineral. Petrology* 150, 70–84.
- Montel J.M., Foret S., Veschambre M., Nicollet C. & Provost A. 1996: Electron microprobe dating of monazite. *Chem. Geol.* 131, 37–53.
- Neubauer F. & Höck V. 2000: Aspects of geology in Austria and adjoining areas: introduction. *Mitt. Österr. Mineral. Gesell.* 92, 7–14.
- Novák M., Uher P., Černý P. & Siman P. 2000: Compositional variations in ferrotapiolite + tantalite pairs from the beryl-columbite pegmatite at Moravany nad Váhom, Slovakia. *Miner. Petrology* 69, 295–306.
- Novák M., Černý P. & Uher P. 2003: Extreme variation and apparent reversal of Nb-Ta fractionation in columbite-group minerals from the Scheibengraben beryl-columbite granitic pegmatite, Maršíkov, Czech Republic. *Eur. J. Mineral.* 15, 565–574.
- Oberli F., Meier M., Berger A., Rosenberg C.L. & Gieré R. 2004: U-Th-Pb and  $^{230}\text{Th}/^{238}\text{U}$  disequilibrium isotope systematics: Precise accessory mineral chronology and melt evolution tracing in the Alpine Bergell intrusion. *Geochim. Cosmochim. Acta* 68, 2543–2560.
- Pamić J. & Balen D. 2001: Tertiary magmatism of the Dinarides and the adjoining south Pannonian Basin: An overview. *Acta Vulcanol.* 13, 9–24.
- Pamić J. & Palinkaš L. 2000: Petrology and geochemistry of Paleogene tonalites from the easternmost parts of the Periadriatic Zone. *Miner. Petrology* 70, 121–141.
- Pamić J., Balen D. & Herak M. 2002: Origin and geodynamic evolution of late Paleogene magmatic associations along the Periadriatic-Sava-Vardar magmatic belt. *Geodinamica Acta* 15, 209–231.
- Peccerillo A. 2005: Plio-Quaternary volcanism in Italy. Petrology, geochemistry, geodynamics. Springer, Berlin, Heidelberg, New York, 1–365.
- Petrík I. & Konečný P. 2009: Metasomatic replacement of inherited metamorphic monazite in a biotite-garnet granite from the Nízke Tatry Mountains, Western Carpathians, Slovakia: Chemical dating and evidence for disequilibrium melting. *Amer. Mineralogist* 94, 957–974.
- Pezzotta F. 2000: Internal structures, parageneses and classification of the miarolitic Li-bearing complex pegmatites of Elba Island (Italy). *Mem. Soc. Ital. Sci. Natur.* 30, 29–43.
- Piccoli P.M. & Candela P.A. 2002: Apatite in igneous systems. In: Kohn M.J., Rakovan J. & Hughes J.M. (Eds.): Phosphates: Geochemical, geobiological and materials importance. *Rev. Mineral. Geochem.* 48, 255–292.
- Pipera K., Koroneos A., Soldatos T., Pécsay Z. & Christofides G. 2013: K/Ar mineral geochronology of the northern part of the Sithonia Plutonic Complex (Chalkidiki, Greece): implications for its thermal history and geodynamic interpretation. *Geol. Carpathica* 64, 133–140.
- Pomella H., Klötzli U., Scholger R., Stipp M. & Fügenschuh B. 2011: The Northern Giudicarie and the Meran-Mauls fault (Alps, Northern Italy) in the light of new paleomagnetic and geochronological data from boudinaged Eo-/Oligocene tonalites. *Int. J. Earth Sci.* 100, 1827–1850.
- Pyle J.M., Spear F.S., Rudnick R.L. & McDonough W.F. 2000: Monazite-xenotime-garnet equilibrium in metapelites and a new monazite-garnet thermometer. *J. Petrology* 42, 2083–2107.
- Ranchin G. 1968: Contribution à l'étude de la répartition de l'uranium à l'état de traces dans les roches granitiques saines les uranites à teneur élevée du Massif de Saint-Sylvestre (Limosin — Massif Central Français). *Sci. Terre* 13, 161–205.
- Rao C., Wang R.C., Hu H. & Zhang W.L. 2009: Complex internal textures in oxide minerals from the Nanping No. 31 dyke of granitic pegmatite, Fujian province, southeastern China. *Canad. Mineralogist* 47, 1195–1212.
- Romer R.L., Schärer U. & Steck A. 1996: Alpine and pre-Alpine magmatism in the root-zone of the western Central Alps. *Contr. Mineral. Petrology* 123, 138–158.
- Sassi R., Mazzoli C., Miller C. & Konzett E. 2004: Geochemistry and metamorphic evolution of the Pohorje Mountain eclogites from the easternmost Austroalpine basement of the Eastern Alps (Northern Slovenia). *Lithos* 78, 235–261.
- Scharbert S. 1975: Radiometrische Altersdaten von Intrusivgesteinen im Raum Eisenkappel (Karawanken, Kärnten). *Verh. Geol. Bundesanst.* 4, 301–304.
- Schärer U., Costa M., Steck A. & Hunziker J. 1996: Termination of major ductile strike-slip shear and differential cooling along the Insubric line (Central Alps): U-Pb, Rb-Sr and  $^{40}\text{Ar}/^{39}\text{Ar}$  ages of cross-cutting pegmatites. *Earth Planet. Sci. Lett.* 142, 331–351.
- Schmid S.M., Fügenschuh B., Kissling E. & Schuster R. 2004: Tectonic map and overall architecture of the Alpine orogen. *Eclogae Geol. Helv.* 97, 93–117.
- Sen J., Ranganath N., Rathaiah Y.V., Sen D.B. & Kak S.N. 2009: Petrography and geochemistry of uranium mineralised Pre-cambrian granitic-pegmatitic rocks of Mawlait, West Khasi Hills District, Meghalaya. *J. Geol. Soc. India* 74, 639–645.
- Soldatos T., Koroneos A., Kamenov B.K., Peytcheva I., von Quadt A., Christofides G., Zheng X. & Sang H. 2008: New U-Pb and Ar-Ar mineral ages for the Barutin-Buynovo-Elatia-Skaloti-Paranesti batholith (Bulgaria and Greece): Refinement of its debatable age. *Geochem. Mineral. Petrology*, (Sofia) 46, 85–102.
- Taylor S.R. & McLennan S.M. 1985: The continental crust: its composition and evolution. Blackwell Scientific Publications, Oxford, 1–307.
- Thöni M. 2002: Sm-Nd isotope systematics in garnet from different lithologies (Eastern Alps): age results and an evaluation of potential problems for garnet Sm-Nd chronometry. *Chem. Geol.* 185, 255–281.
- Thöni M., Miller C., Blichert-Toft J., Whitehouse M.J., Konzett J. & Zanetti A. 2008: Timing of high-pressure metamorphism and exhumation of the eclogite type-locality (Kupplerbrunn-Prickler Halt, Saualpe, south-eastern Austria): Constraints from correlations of the Sm-Nd, Lu-Hf, U-Pb and Rb-Sr isotopic systems. *J. Metamorph. Geology* 26, 561–581.
- Tindle A.G. & Breaks F.W. 1998: Oxide minerals of the Separation

- Rapids rare-element granitic pegmatite group, northwestern Ontario. *Canad. Mineralogist* 36, 609–636.
- Trajanova M., Pécskay Z. & Itaya T. 2008: K-Ar geochronology and petrography of the Miocene Pohorje Mountains batholith (Slovenia). *Geol. Carpathica* 59, 247–260.
- Uher P. & Černý P. 1998: Zircon in Hercynian granitic pegmatites of the Western Carpathians, Slovakia. *Geol. Carpathica* 49, 261–270.
- Van Lichtervelde M., Salvi S., Beziat D. & Linnen R.L. 2007: Textural features and chemical evolution in tantalum oxides: magmatic versus hydrothermal origins for Ta mineralization in the Tanco Lower Pegmatite, Manitoba, Canada. *Econ. Geol.* 102, 257–276.
- Vrabec M. & Dolenc T. 2002: Some genetic characteristics of pegmatite veins from the Pohorje Mountains (Slovenia). *Gold-schmidt Conference Abstr.*, A811.
- Vrabec M., Janák M., Froitzheim N. & de Hoog C.J. 2012: Phase relations during peak metamorphism and decompression of the UHP kyanite eclogites, Pohorje Mountains (Eastern Alps, Slovenia). *Lithos* 144, 40–55.
- Wenger M. & Armbruster T. 1991: Columbite  $(\text{Fe}, \text{Mn})(\text{Nb}, \text{Ta})_2\text{O}_6$  in the pegmatites of the calc-alkaline Bergell intrusion (south-east Central Alps). *Schweiz. Mineral. Petrogr. Mitt.* 71, 249–369.
- Whitworth M.P. 1992: Petrogenetic implications of garnets associated with lithium pegmatites from SE Ireland. *Mineral. Mag.* 56, 75–83.
- Wise M.A. & Brown C.D. 2010: Mineral chemistry, petrology and geochemistry of the Sebago granite-pegmatite system, southern Maine, USA. *J. Geosci.* 55, 3–26.
- Wise M.A., Francis C.A. & Černý P. 2012: Compositional and structural variations in columbite-group minerals from granitic pegmatites of the Brunswick and Oxford fields, Maine: differential trends in F-poor and F-rich environments. *Canad. Mineralogist* 50, 1515–1530.
- Zupančič N., Dobnikar M. & Dolenc T. 1994: Determination of beryl in pegmatite veins from the igneous rock of the Pohorje Mountains. In: Leban I. (Ed.): Third Slovenian-Croatian crystallographic meeting, Kranjska gora, 29–30 September 1994. Book of abstracts, Programme. *Laboratory for Inorganic Chemistry, Department of Chemistry and Chemical Technology*, Ljubljana, 51.